Computers and Structures 223 (2019) 106101

Contents lists available at ScienceDirect

Computers and Structures

journal homepage: www.elsevier.com/locate/compstruc

On the best choice of symmetry group for group-theoretic computational schemes in solid and structural mechanics

Alphose Zingoni

Department of Civil Engineering, University of Cape Town, Rondebosch 7701, Cape Town, South Africa

ARTICLE INFO

Article history:
Received 5 January 2019
Accepted 23 July 2019

Keywords:
Symmetry
Group theory
Symmetry group
Eigenvalue problem
Vibration
Mode shape

ABSTRACT

Group theory has been used for many years to study phenomena in various branches of physics and chemistry, such as quantum mechanics, crystallography and molecular structure. Within engineering mechanics, it has found application in simplifying the analysis of systems exhibiting symmetry properties, and has been particularly effective in studying vibration, bifurcation and kinematic phenomena. Symmetry properties of physical systems are described by symmetry groups. Given a physical system with multiple symmetry properties, the question arises as to which of the various possible symmetry groups is the most appropriate for computational purposes. This question is particularly relevant for configurations belonging to symmetry groups of high order, which typically are associated with several subgroups. The aim of this paper is to highlight the computational implications of choice of symmetry group, and to present, for the first time, a rational criterion for identifying the most computationally efficient symmetry group for a given problem. The criterion is applied to the problem of a cubic configuration with octahedral symmetry.

1. Introduction

Group theory is a powerful tool in the analysis of physical systems exhibiting symmetry properties [1]. Early applications of group theory arose in various branches of physics and chemistry, such as crystallography, molecular structure and quantum mechanics, where symmetry abounds [2–5]. Group theory has proved to be very effective in studying physical phenomena in complex molecules, such as the vibration of the carbon-60 molecule [6].

Within the field of engineering mechanics, it has been long recognised that symmetry has a significant influence on the behaviour of a system, and that symmetry can be exploited to simply the analysis of the system. Among the earliest applications of group theory to problems in structural mechanics was the buckling of symmetrical frameworks [7]. Since then, bifurcation theory has emerged as one of the most fruitful areas of application of group-theoretic methods in structural mechanics [8–12]. Although wider in scope, group theory has come to be regarded as the "mathematics of symmetry" [13], owing to its unique suitability in accounting for all physical phenomena associated with symmetry. Group theory has been successfully used to simplify the static analysis of symmetric space frames [14], the decomposition of load systems [15,16], and the study of rigidity and finite mechanisms in skeletal structures [17–24]. Almost 25 years ago, the author and co-investigators [14] presented a group-theoretic formulation for the flexibility analysis of multi-storey space frames, and went on to show how arbitrary loads on a symmetric structure can be decomposed for allocation to the symmetry-adapted subspaces of the relevant symmetry group [15]. Since then, applications of group theory have been extended to many other structural problems.

Group theory has proved to be particularly suitable for studying problems of the vibration of symmetric structures [25–38], which have included spring-mass dynamic systems [32,33], plane grids and layered space grids [27,31], cable-net systems [28,37,38], plates [35] and shells [29]. Among the author's early contributions in the area of vibration analysis were a group-theoretic symbolic formulation for the computation of natural frequencies of rectangular and square plane grids [27], and the formulation of a group-theoretic computational scheme for the vibration analysis of high-tension cable nets [28]. The latter work has recently been extended to cable nets of more complex symmetry [37,38]. The author has also employed group theory to study the small transverse vibrations of layered space grids [31], allowing a deeper understanding of the character of the modes for various grid configurations (triangular and hexagonal layouts included). In another study [33], it was shown how certain rectilinear spring-mass

E-mail address: alphose.zingoni@uct.ac.za

https://doi.org/10.1016/j.compstruc.2019.106101
0045-7949/

dynamical systems with no apparent symmetry properties can be converted into equivalent symmetric configurations, and group theory then applied to simplify the calculation of their natural frequencies. Based on group-theory, a finite-difference formulation for the vibration analysis of symmetric plates has also been presented [35]. Some of these formulations may be seen in a recent book on linear vibration analysis [36], which also includes a concise treatment of symmetry, symmetry groups and group representation theory.

Group theory has also been employed by Kaveh and Nikbakht [39] to study the stability of skeletal structures. As Kaveh and other investigators have shown, symmetric and repetitive structures may also been studied using the related techniques of graph theory [40–42], or a combination of group theory and graph theory [34,43–45].

With application to finite-element analysis in mind, several investigators (including the author) have developed formulations that utilize concepts of symmetry and group theory to simplify particular levels of the finite element method [46–51]. At element level, group theory has been used to decompose the displacement field of truss and beam finite elements [46] as well as solid hexahedral finite elements [48–50], in all cases leading to considerable simplifications in the calculation of associated element matrices. At structural level, group-theory has been employed to achieve simplifications in the buckling analysis of plates and shells [47], and in the dynamic analysis of symmetric finite-element models [51].

Since symmetry is not always easy to identify (particularly in complex structures), a significant amount of effort has also been directed towards developing procedures for the automatic recognition of symmetry [52–55]. Not only does group theory reduce computational effort, but it also provides valuable insights on the behaviour of a physical system [23,31,56,57].

It should be clarified right from the outset that in the present context, use of group theory to tackle problems involving symmetry is not aimed at increasing the accuracy of the solution. Rather, and as demonstrated in previous studies of the author, the merits of the procedure lie in the computational simplications that are achieved when the vector space of the problem is decomposed into several symmetry-adapted subspaces, as well as the insights on the physical behaviour of the system that are gained. In the context of vibration analysis, some of these insights include the prediction of the symmetry types of all the vibration modes before any detailed analysis is undertaken, the prediction of the existence of doubly-occurring frequencies, a better understanding of the nature of the modes (type of symmetries) associated with these repeating frequencies, and a prediction of points, lines and planes of stationary nodes (knowledge of which can be valuable when it is required to decide the best locations for the placement or installation of vibration-sensitive equipment).

In itself, group-theoretic decomposition is a mathematically exact process, therefore as long as the basic structural theory is correct, the results of group-theoretic simplifications will also be correct. So while group-theoretic computations do not increase the accuracy of the solution, they can certainly make the calculations simpler and faster through the vector-space decomposition. It might be argued that vector-space decomposition is not necessary since computers can do an analysis quite quickly in the full space of the problem, but the real merit of group-theoretic decompositions becomes evident in the case of large-scale problems with millions of unknowns or degrees of freedom, where huge computational effort is involved, and simplifications are desirable. For such problems, the splitting of the computations into subspaces of smaller dimension also lends itself to the use of parallel processors, which would speed up computations even further.

A system or an object is said to exhibit symmetry if it can be turned into one or more new configurations physically indistinguishable from the initial configuration through the application of one or more symmetry operations. Symmetry operations include reflections in planes, rotations about axes, or inversions through the centre. This broad definition of symmetry encompasses the more conventional concepts of bilateral symmetry (where a structural configuration has two axes or two planes of symmetry that are perpendicular to each other) and cyclic symmetry (where a structural configuration has one axis of rotational symmetry and a finite number of rotational symmetry operations about this axis). Configurations exhibiting bilateral symmetry and cyclic symmetry are therefore covered by present considerations. There is also a related class of problems called *repeated* structures, where identical structural units repeat in one or more directions, or around a given axis. Unless these structures also exhibit symmetry in the sense already defined, they will not be the subject of present considerations, which is solely concerned with symmetric structures.

A set of elements $\{\alpha,\beta,\gamma,\ldots,\sigma,\ldots\}$ comprises a group G if the following axioms are satisfied:

(i) the product γ of any two elements α and β of the group, which is given by $\gamma = \alpha\beta$, is a unique element which also belongs to the group.
(ii) among the elements of G, there is an identity element e which, when multiplied with any element α of the group, leaves the element unchanged: $e\alpha = \alpha e = \alpha$.
(iii) each element α of G has an inverse α^{-1} also belonging to the group, such that $\alpha\alpha^{-1} = \alpha^{-1}\alpha = e$.
(iv) when three or more elements of G are multiplied, the order of the multiplication does not affect the result: $\alpha(\beta\gamma) = (\alpha\beta)\gamma$.

A group where all elements are symmetry operations constitutes a symmetry group. Symmetry operations may be reflections in planes of symmetry (denoted by σ_l, where l is the plane of symmetry), rotations about an axis of symmetry (denoted by C_n, if the angle of rotation is $2\pi/n$), rotary-reflections S_n (denoting a rotation through an angle $2\pi/n$, combined with a reflection in the plane perpendicular to the rotation axis), or inversions i (which are reflections in the centre of symmetry, that is, the one point of a space object which is unmoved by all symmetry operations). Clearly, an inversion is equivalent to a rotary-reflection of angle of rotation π. In all our considerations, we will assume that all planes of symmetry are vertical, unless otherwise stated, hence we will denote reflection planes by the symbol v instead of l.

Classification of symmetry groups is usually based on the types of symmetry elements making them up. Groups denoted by C_n and C_{nv} all possess a single n-fold axis of rotational symmetry; they are of *order* n and $2n$ respectively, the order of a group being simply the total number of elements comprising it. Thus, each of these groups possesses n rotation elements (one of which is actually the identity element e), with the C_{nv} family having an additional n reflection elements. Groups denoted by D_n and D_{nh} have one n-fold axis of rotational symmetry and horizontal C_2 axes, with the D_{nh} family also having a horizontal plane of reflection. Groups T_h, O_h and I_h denote tetrahedral, octahedral and icosahedral groups respectively, and are associated with regular polyhedra with more than one n-fold axis of symmetry. These are not the only types of symmetry groups; there are several other types.

Fig. 1 shows nodal configurations with the symmetries of (a) a square, (b) a regular hexagon, (c) a right prism with a base in the form of a regular hexagon, and (d) a cube. The arrows indicate displacement or force vectors associated with these nodes, with positive directions chosen to comply with the full symmetry of the nodal configuration. The symmetry groups of these four configurations, with some of their subgroups (a subgroup being simply a group whose elements are a subset of the elements of the parent group) given in brackets, are as follows:

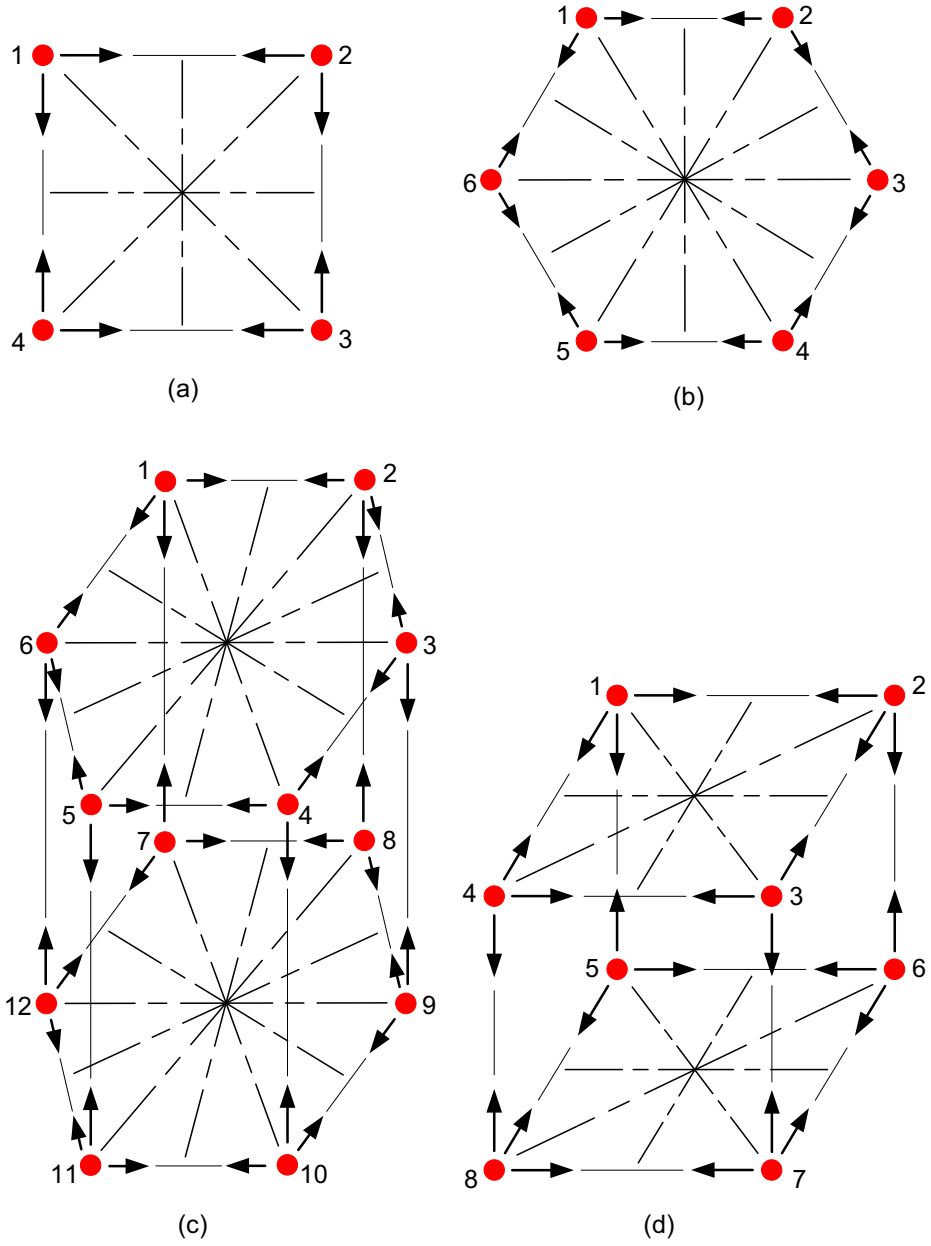

Fig. 1. Nodal configurations with various symmetries: (a) square (C_{4v} symmetry); (b) regular hexagon (C_{6v} symmetry); (c) right prism with a base in the form of a regular hexagon (D_{6h} symmetry); (d) cube (O_h symmetry).

(a) C_{4v} (C_{2v}, C_{1v})
(b) C_{6v} (C_{3v}, C_{1v})
(c) D_{6h} (D_{3h}, C_{6v}, C_{3v}, C_{1v})
(d) O_h (O, D_{4h}, D_{2h}, C_{4v}, C_{2v}, C_{1v})

The symmetry groups C_{4v}, C_{6v}, D_{6h} and O_h are of order 8, 12, 24 and 48 respectively, the order of a symmetry group being the number of symmetry elements it has. In describing the symmetry of a given structural configuration, the full symmetry group (taking into account all the symmetry of the configuration) or any of its subgroups (accounting for only some of the symmetry) may be used. An example, the configuration in Fig. 1(a) may be analysed on the basis of the symmetry group C_{4v} (which takes into account all the symmetry) or on the basis of the subgroup C_{2v} (which takes into account only some of the symmetry).

Given a physical system with multiple symmetry properties, the question arises as to which of the various possible symmetry groups is the most efficient for computational purposes. This is a very important question which hardly seems to have been addressed in the literature on group-theoretic formulations in solid and structural mechanics. The question is particularly relevant to configurations belonging to symmetry groups of high order, which typically are associated with several subgroups. The aim of this paper is to highlight the computational implications of choice of symmetry group, and present a rational criterion for identifying the most computationally efficient symmetry group for a given problem.

We begin, in Section 2, by explaining some key concepts on the basis of symmetry groups C_{2v} and C_{4v}. These groups are applicable to many practical layouts of plane grids, space grids, cable-net roofs and plates, which are usually of rectangular plan form (the square being a special case). After stating the elements of groups C_{2v} and C_{4v}, we introduce the concept of an *idempotent*, and presents the idempotents for these groups. These are central to group-theoretic computations.

In Section 3, we consider a 16-node lumped-mass dynamic system of C_{4v} symmetry as a case study. The system is general, and may represent a plane grid, a space grid, a prestressed cable net, a plate or any other structural system having this configuration in plan, and experiencing small transverse vibrations. We tackle the problem on the basis of both symmetry groups C_{2v} and C_{4v}, from the derivation of symmetry-adapted freedoms (subspace basis vectors) and the calculation of symmetry-adapted flexibility coefficients, to the setting up of the characteristic equations that yield the eigenvalues (i.e. natural frequencies of vibration) of the system. In this way, the computational implications of using either of these symmetry groups are clearly illustrated.

An added benefit of the treatment is the presentation of a rigorous derivation of subspace flexibility matrices from an arbitrary set of conventional flexibility coefficients. The formulation is applied to the numerical example of the small transverse vibrations of a plane grid, and the symmetry group C_{2v} selected in computing all natural frequencies and mode shapes of the system.

In Section 4, we go back to the general situation of a physical configuration whose symmetry can be described by a number of alternative symmetry groups, and propose a simple criterion for identifying the best symmetry group for computational purposes. The criterion is applied to the cubic configuration of Fig. 1(d), allowing some important conclusions to be made. Preliminary findings were presented at the Thirteenth International Conference on Computational Structures Technology in Barcelona [58], but without the detailed derivations and analysis that now appear in this paper.

2. Some properties of symmetry groups C_{2v} and C_{4v}

2.1. Symmetry elements

The symmetry group C_{2v} describes the symmetry of a rectangular configuration. Let us take the configuration to lie in the xy plane, with the coordinate directions $\{x, y\}$ being parallel to the sides of the rectangle, and the origin O being at the centre of the configuration. The z axis is perpendicular to the xy plane and passes through O. With reference to this coordinate system, the symmetry elements of group C_{2v} may be described are as follows:

e: identity element
C_2: rotation through an angle of $\pi/2$ about the z axis
σ_x: reflection in the vertical xz plane
σ_y: reflection in the vertical yz plane

The symmetry group C_{4v}, describing the symmetry properties of a square, has all the above four symmetry elements. In addition, it also has the following symmetry elements, where the subscripts 1 and 2 refer to the two diagonals 1-1 and 2-2 of the square:

C_4: clockwise rotation through an angle of $\pi/4$ about the z axis
C_4^{-1}: anticlockwise rotation through an angle of $\pi/4$ about the z axis
σ_1: reflection in the vertical diagonal plane containing the diagonal 1-1 and the z axis
σ_2: reflection in the vertical diagonal plane containing the diagonal 2-2 and the z axis

Thus the symmetry groups C_{2v} and C_{4v} are of order 4 and 8 respectively, the order of a group being the number of symmetry elements making up the group.

In the next section, we will briefly explain the concept of an idempotent, which is central to group-theoretic decomposition. For a detailed treatment of other important concepts leading to this (such as the classes of a group, class sums, group representations, characters, irreducible representations, character tables, group algebra), the reader may refer to some of the earlier work of the author [28], or books on application of group theory to physical [1] and structural-engineering problems [25,36].

2.2. Idempotents

According to representation theory of symmetry groups [1–5], *idempotents* $P^{(i)}$ of the group algebra are its non-zero elements which satisfy the relation $\{P^{(i)}\}^2 = P^{(i)}$. Orthogonal idempotents satisfy the relation $P^{(i)}P^{(j)} = 0$ if $i \neq j$. They are linearly independent; the sum of orthogonal idempotents is also an idempotent. Idempotents of the centre of the group algebra are linear combinations of class sums. An idempotent $P^{(i)}$ corresponding to the irreducible representation $R^{(i)}$, by operating on vectors of the space V, nullifies every vector which does not belong to the subspace $S^{(i)}$ of $R^{(i)}$. Thus, out of all the vectors belonging to the group-invariant subspaces $S^{(1)}$, $S^{(2)}$,...,$S^{(k)}$, the operator $P^{(i)}$ selects all vectors belonging to the subspace $S^{(i)}$, and therefore acts as a *projection operator* [1] of the subspace $S^{(i)}$. The orthogonal idempotents of the centre of the group algebra ($P^{(i)}$ for subspace $S^{(i)}$; $i = 1,2,...k$) can be written down directly from the character table using the relation

$$P^{(i)} = \frac{h_i}{h} \sum_{\sigma} \chi_i(\sigma^{-1})\sigma \tag{1}$$

where h is the order of G (i.e. the number of elements of G), h_i is the dimension of the ith irreducible representation (given by $h_i = \chi_i(e)$, the first character of the ith row of the character table), χ_i is a character of the ith irreducible representation, σ is an element of G, and σ^{-1} its inverse. The idempotents for groups C_{2v} and C_{4v} are obtained as follows [28,31,36,57]:

Group C_{2v}

$$P^{(1)} = \frac{1}{4}(e + C_2 + \sigma_x + \sigma_y) \tag{2a}$$

$$P^{(2)} = \frac{1}{4}(e + C_2 - \sigma_x - \sigma_y) \tag{2b}$$

$$P^{(3)} = \frac{1}{4}(e - C_2 + \sigma_x - \sigma_y) \tag{2c}$$

$$P^{(4)} = \frac{1}{4}(e - C_2 - \sigma_x + \sigma_y) \tag{2d}$$

Group C_{4v}

$$P^{(1)} = \frac{1}{8}\left(e + C_4 + C_4^{-1} + C_2 + \sigma_x + \sigma_y + \sigma_1 + \sigma_2\right) \tag{3a}$$

$$P^{(2)} = \frac{1}{8}\left(e + C_4 + C_4^{-1} + C_2 - \sigma_x - \sigma_y - \sigma_1 - \sigma_2\right) \tag{3b}$$

$$P^{(3)} = \frac{1}{8}\left(e - C_4 - C_4^{-1} + C_2 + \sigma_x + \sigma_y - \sigma_1 - \sigma_2\right) \tag{3c}$$

$$P^{(4)} = \frac{1}{8}\left(e - C_4 - C_4^{-1} + C_2 - \sigma_x - \sigma_y + \sigma_1 + \sigma_2\right) \tag{3d}$$

$$P^{(5A)} = \frac{1}{4}(e - C_2 + \sigma_1 - \sigma_2) \tag{3e}$$

$$P^{(5B)} = \frac{1}{4}(e - C_2 - \sigma_1 + \sigma_2) \tag{3f}$$

3. A lumped-mass dynamic system of C_{4v} symmetry

3.1. Problem description

Fig. 2(a) shows the horizontal projection of a 16-node lumped-mass dynamic system whose arrangement of supports, members and masses conforms to the symmetry group C_{4v} (i.e. the pattern of members, nodes and supports has the symmetry of a square). The system is experiencing small transverse vibrations at the nodal locations; we will denote the associated transverse displacements by w_i ($i = 1,2,\ldots,16$). Consistent with the usual assumptions of lumped-parameter models, the members are assumed to be "massless", their role being simply to provide the restoring forces necessary to sustain the transverse vibrations; all the mass of the system is assumed to be concentrated at the nodes. For the purposes of this discussion, we will ignore the effects of damping.

This physical system is quite general, and may represent (i) a plane grid of rigidly connected members (the vertical restoring forces being provided by the flexural stiffnesses of the grid members), (ii) a double-layer space grid of pin-jointed truss members (the vertical components of the axial forces of the space grid providing the restoring forces), (iii) a tightly stretched shallow cable net (the vertical components of the cable prestress forces providing the restoring forces) (iv) a relatively light square plate carrying a regular array of heavy pieces of machinery (such as pumps or electric motors) at specific locations (the restoring forces being the flexural rigidity of the plate).

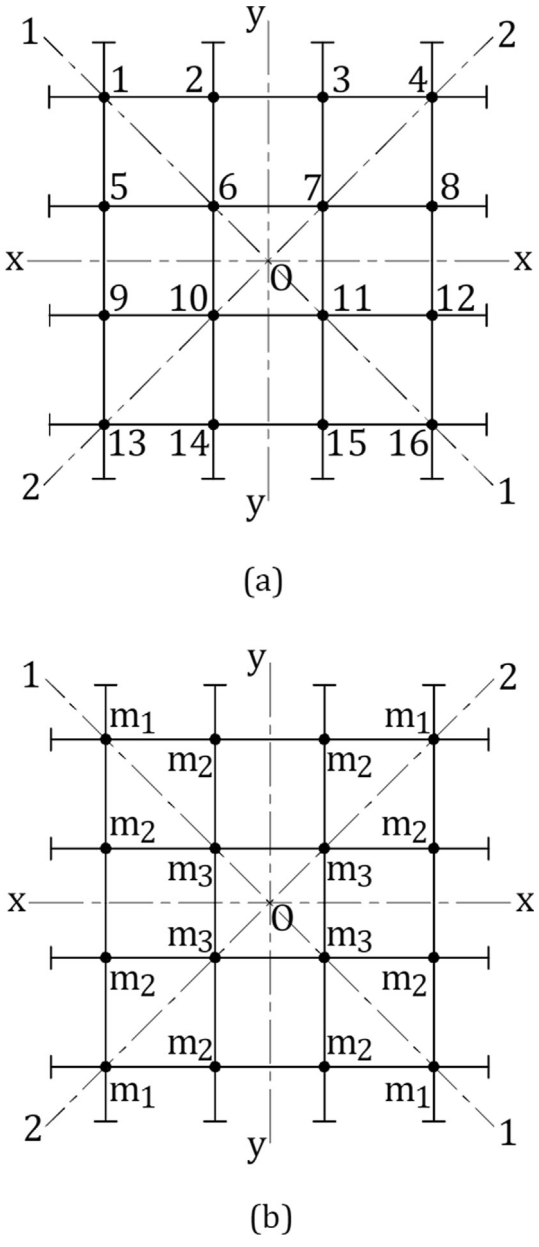

Fig. 2. A 16-node dynamic system with C_{4v} symmetry: (a) node numbering and reference axes; (b) values of masses at the nodes.

Let the nodes of the system be numbered from 1 to 16 as shown. The centre of symmetry of the configuration is the point O in the diagram. The four reference axes of symmetry are the coordinate axes x-x and y-y, and the diagonal axes 1-1 and 2-2. The symmetry operations of group C_{4v}, when applied on the nodal positions 1–16 of the configuration, yield three permutation sets: corner nodes {1,4,13,16}, mid-side nodes {2,3,5,8,9,12,14,15}, and centre nodes {6,7,10,11}. Consistent with the requirements of C_{4v} symmetry, each node of a given permutation set will be modelled with the same mass. The equal masses assigned to each of the three sets of nodes are denoted by $\{m_1,m_2,m_3\}$ as illustrated in Fig. 2(b). The pattern of these is, of course, of symmetry C_{4v}.

Conventional vibration analysis of the physical system results in an eigenvalue problem of dimension n, where for our example $n = 16$. The characteristic equation is a 16-th degree polynomial equation whose roots are the 16 eigenvalues of the problem, which are, of course, the 16 natural frequencies of vibration of the system. Substitution of each eigenvalue into the eigenvector equation yields the associated eigenvector, which is the mode shape corresponding to the natural frequency in question. All these calculations require a considerable amount of effort. Owing to symmetry, group-theory allows the 16-dimensional vector space of the problem to be decomposed into k independent subspaces each of dimension n_i ($i = 1,2,\ldots,k$), where $n_i < n$ and $n_1 + n_2 + \ldots + n_k = n$. The eigenvalues calculated within these smaller subspaces are, in fact, the eigenvalues of the original problem. This is why group-theoretic decomposition results in considerable reductions in computational effort in comparison with a conventional analysis of the physical system. If more than one symmetry group is applicable, the reduction in computational effort depends on the symmetry group that is adopted in modelling the behaviour of the system.

While the full symmetry of the 16-node configuration of Fig. 2(a) is described by the symmetry group C_{4v}, it is clear that the subgroup C_{2v} is also applicable, although it is not able to account for all the symmetry properties of the configuration. However, the fact that the group C_{4v} can account for all the symmetry of the configuration does not automatically mean that it is computationally more efficient than group C_{2v} in calculating the natural frequencies (eigenvalues) and mode shapes (eigenvectors) of the system. In the next section, we explore this issue further, by assembling the eigenvalue equations of the system on the basis of both groups C_{2v} and C_{4v}, and comparing the results. It is also evident that the very simple group C_{1v}, with elements e (identity) and σ_x (reflection in the xz plane), also applies, but with only two idempotents $P^{(1)} = 1/2(e + \sigma_x)$ and $P^{(2)} = 1/2(e - \sigma_x)$ corresponding to the symmetric and antisymmetric subspaces respectively, this group is clearly too inefficient for the configuration of Fig. 2(a), and will not be pursued.

3.2. Symmetry-adapted freedoms

To generate the symmetry-adapted freedoms of a given subspace of the 16-node example, we apply the idempotent of the subspace to each of the 16 degrees of freedom of the system. We then select any set of linearly independent symmetry-adapted freedoms as the basis vectors spanning that subspace. In writing down the

basis vectors, we do not need to include scalar multipliers such as 1/4 or 1/8. We repeat this for all subspaces of the problem, each time using the correct idempotent for the subspace in question. Considering each of the groups C_{2v} and C_{4v} separately, we obtain the following results for the basis vectors of the 16-node configuration of Fig. 2(a):

Symmetry Group C_{2v}

Basis vectors for subspace $S^{(1)}$

$$\Phi_1^{(1)} = w_1 + w_{16} + w_{13} + w_4 \tag{4a}$$

$$\Phi_2^{(1)} = w_2 + w_{15} + w_{14} + w_3 \tag{4b}$$

$$\Phi_3^{(1)} = w_5 + w_{12} + w_9 + w_8 \tag{4c}$$

$$\Phi_4^{(1)} = w_6 + w_{11} + w_{10} + w_7 \tag{4d}$$

Basis vectors for subspace $S^{(2)}$

$$\Phi_1^{(2)} = w_1 + w_{16} - w_{13} - w_4 \tag{5a}$$

$$\Phi_2^{(2)} = w_2 + w_{15} - w_{14} - w_3 \tag{5b}$$

$$\Phi_3^{(2)} = w_5 + w_{12} - w_9 - w_8 \tag{5c}$$

$$\Phi_4^{(2)} = w_6 + w_{11} - w_{10} - w_7 \tag{5d}$$

Basis vectors for subspace $S^{(3)}$

$$\Phi_1^{(3)} = w_1 - w_{16} + w_{13} - w_4 \tag{6a}$$

$$\Phi_2^{(3)} = w_2 - w_{15} + w_{14} - w_3 \tag{6b}$$

$$\Phi_3^{(3)} = w_5 - w_{12} + w_9 - w_8 \tag{6c}$$

$$\Phi_4^{(3)} = w_6 - w_{11} + w_{10} - w_7 \tag{6d}$$

Basis vectors for subspace $S^{(4)}$

$$\Phi_1^{(4)} = w_1 - w_{16} - w_{13} + w_4 \tag{7a}$$

$$\Phi_2^{(4)} = w_2 - w_{15} - w_{14} + w_3 \tag{7b}$$

$$\Phi_3^{(4)} = w_5 - w_{12} - w_9 + w_8 \tag{7c}$$

$$\Phi_4^{(4)} = w_6 - w_{11} - w_{10} + w_7 \tag{7d}$$

Symmetry Group C_{4v}

Basis vectors for subspace $S^{(1)}$

$$\Phi_1^{(1)} = w_1 + w_4 + w_{13} + w_{16} \tag{8a}$$

$$\Phi_2^{(1)} = w_2 + w_3 + w_5 + w_8 + w_9 + w_{12} + w_{14} + w_{15} \tag{8b}$$

$$\Phi_3^{(1)} = w_6 + w_7 + w_{10} + w_{11} \tag{8c}$$

Basis vector for subspace $S^{(2)}$

$$\Phi_1^{(2)} = w_2 - w_3 - w_5 + w_8 + w_9 - w_{12} - w_{14} + w_{15} \tag{9}$$

Basis vector for subspace $S^{(3)}$

$$\Phi_1^{(3)} = w_2 + w_3 - w_5 - w_8 - w_9 - w_{12} + w_{14} + w_{15} \tag{10}$$

Basis vectors for subspace $S^{(4)}$

$$\Phi_1^{(4)} = w_1 - w_4 - w_{13} + w_{16} \tag{11a}$$

$$\Phi_2^{(4)} = w_2 - w_3 + w_5 - w_8 - w_9 + w_{12} - w_{14} + w_{15} \tag{11b}$$

$$\Phi_3^{(4)} = w_6 - w_7 - w_{10} + w_{11} \tag{11c}$$

Basis vectors for subspace $S^{(5A)}$

$$\Phi_1^{(5A)} = w_1 - w_{16} \tag{12a}$$

$$\Phi_2^{(5A)} = w_6 - w_{11} \tag{12b}$$

$$\Phi_3^{(5A)} = w_2 + w_5 - w_{12} - w_{15} \tag{12c}$$

$$\Phi_4^{(5A)} = w_3 - w_8 + w_9 - w_{14} \tag{12d}$$

Basis vectors for subspace $S^{(5B)}$

$$\Phi_1^{(5B)} = w_4 - w_{13} \tag{13a}$$

$$\Phi_2^{(5B)} = w_7 - w_{10} \tag{13b}$$

$$\Phi_3^{(5B)} = w_3 + w_8 - w_9 - w_{14} \tag{13c}$$

$$\Phi_4^{(5B)} = w_2 - w_5 + w_{12} - w_{15} \tag{13d}$$

Thus, use of group C_{2v} decomposes the vector space of the original problem (which is of dimension $n = 16$) into four subspaces of dimensions $n_i = \{4,\ 4,\ 4,\ 4\}$. On the other hand, use of group C_{4v} decomposes the problem into six subspaces of dimensions $n_i = \{3,\ 1,\ 1,\ 3,\ 4,\ 4\}$. Although the decomposition achieved by the use of group C_{4v} is of higher degree than that achieved by the use of group C_{2v}, the more equitable decomposition yielded by group C_{2v} may very well weigh in favour of the adoption of this group. For large-scale problems, where parallel processors are often employed to handle the calculations within the independent subspaces, a more uniform spread of computational effort across the various subspaces is particularly desirable.

3.3. Conventional flexibility matrix

In this treatment, we will adopt the flexibility formulation (as opposed to the stiffness formulation) of the eigenvalue problem. The conventional flexibility matrix for the 16-node configuration of Fig. 2(a) consists of elements $f_{i,j}$ (i = 1,2,...,16; j = 1,2,...,16)), where $f_{i,j}$ is the vertical deflection at node i due to a unit vertical force applied at node j.

First consider the situation of a unit vertical force applied at Node 1. Regardless of whether the configuration is a grid, a plate, a cable net or some other structure, we will have a total of *ten* distinct vertical deflections (i.e. values of flexibility coefficients) at Nodes 1–16, owing to the symmetry of the physical configuration. Flexibility coefficients for a specific problem (a grid, a cable net, a plate, etc.) can readily be calculated based on an appropriate theory for the problem in question, hence we will assume these are known quantities. This also allows us to proceed without loss of generality. Let us denote these (known) flexibility coefficients by $a_1,\ a_2,\ \ldots,\ a_{10}$ as follows:

$$f_{1,\,1} = a_1 \tag{14a}$$

$$f_{2,\,1} = f_{5,\,1} = a_2 \tag{14b}$$

$$f_{3,\,1} = f_{9,\,1} = a_3 \tag{14c}$$

$$f_{4,1} = f_{13,1} = a_4 \tag{14d}$$

$$f_{6,1} = a_5 \tag{14e}$$

$$f_{7,1} = f_{10,1} = a_6 \tag{14f}$$

$$f_{8,1} = f_{14,1} = a_7 \tag{14g}$$

$$f_{11,1} = a_8 \tag{14h}$$

$$f_{12,1} = f_{15,1} = a_9 \tag{14i}$$

$$f_{16,1} = a_{10} \tag{14j}$$

Nodes 4, 13 and 16 belong to the same permutation set as Node 1. Therefore the effects (i.e. vertical deflections) when the unit vertical force is applied at Node 4, at Node 13 and at Node 16 may be deduced directly from the results for Node 1.

Next, consider the situation of a unit vertical force applied at Node 2. From the well-known property of the flexibility matrix that $f_{i,j} = f_{j,i}$, and further considerations of symmetry, the vertical deflections at Nodes 1, 4, 13 and 16 are related to the quantities in Eq. (14) as follows:

$$f_{1,2} = f_{2,1} = a_2 \tag{15a}$$

$$f_{4,2} = f_{2,4} = f_{3,1} = a_3 \tag{15b}$$

$$f_{13,2} = f_{2,13} = f_{8,1} = a_7 \tag{15c}$$

$$f_{16,2} = f_{2,16} = f_{12,1} = a_9 \tag{15d}$$

The vertical deflections at the remaining twelve nodes of Fig. 2(a), resulting from the application of a unit vertical force at Node 2, will be different from the values in Eq. (14). These flexibility coefficients will be denoted by a_{11}, a_{12}, ..., a_{21} (all assumed to be known quantities) as follows:

$$f_{2,2} = a_{11} \tag{16a}$$

$$f_{3,2} = a_{12} \tag{16b}$$

$$f_{5,2} = a_{13} \tag{16c}$$

$$f_{6,2} = a_{14} \tag{16d}$$

$$f_{7,2} = a_{15} \tag{16e}$$

$$f_{8,2} = a_{16} \tag{16f}$$

$$f_{9,2} = f_{2,8} = f_{8,2} = a_{16} \tag{16g}$$

$$f_{10,2} = a_{17} \tag{16h}$$

$$f_{11,2} = a_{18} \tag{16i}$$

$$f_{12,2} = a_{19} \tag{16j}$$

$$f_{14,2} = a_{20} \tag{16k}$$

$$f_{15,2} = a_{21} \tag{16l}$$

Nodes {3, 5, 8, 9, 12, 14, 15} belong to the same permutation set as Node 2. Therefore the effects (i.e. vertical deflections) when the unit vertical force is applied at each of these nodes in turn may be deduced directly from the results for Node 2.

Finally, consider the situation of a unit vertical force applied at Node 6. The vertical deflections at the central nodes (i.e. Nodes 6, 7, 10 and 11) will be distinct from the values in Eqs. (14) and (16). These flexibility coefficients will be denoted by a_{22}, a_{23} and a_{24} (all assumed to be known quantities) as follows:

$$f_{6,6} = a_{22} \tag{17a}$$

$$f_{7,6} = f_{10,6} = a_{23} \tag{17b}$$

$$f_{11,6} = a_{24} \tag{17c}$$

Nodes {7, 10, 11} belong to the same permutation set as Node 6. Therefore the effects (i.e. vertical deflections) when the unit vertical force is applied at each of these nodes in turn may be deduced directly from the results for Node 6.

The remaining flexibility coefficients of the problem follow from the relationship $f_{i,j} = f_{j,i}$, where all the $f_{j,i}$ are already defined above. The 16×16 conventional flexibility matrix A of the structural configuration shown in Fig. 2(a) may be fully written out in terms of the *twenty-four* distinct values of the flexibility coefficients as follows:

$$A = \begin{bmatrix}
a_1 & a_2 & a_3 & a_4 & a_2 & a_5 & a_6 & a_7 & a_3 & a_6 & a_8 & a_9 & a_4 & a_7 & a_9 & a_{10} \\
a_2 & a_{11} & a_{12} & a_3 & a_{13} & a_{14} & a_{15} & a_{16} & a_{16} & a_{17} & a_{18} & a_{19} & a_7 & a_{20} & a_{21} & a_9 \\
a_3 & a_{12} & a_{11} & a_2 & a_{16} & a_{15} & a_{14} & a_{13} & a_{19} & a_{18} & a_{17} & a_{16} & a_9 & a_{21} & a_{20} & a_7 \\
a_4 & a_3 & a_2 & a_1 & a_7 & a_6 & a_5 & a_2 & a_9 & a_8 & a_6 & a_3 & a_{10} & a_9 & a_7 & a_4 \\
a_2 & a_{13} & a_{16} & a_7 & a_{11} & a_{14} & a_{17} & a_{20} & a_{12} & a_{15} & a_{18} & a_{21} & a_3 & a_{16} & a_{19} & a_9 \\
a_5 & a_{14} & a_{15} & a_6 & a_{14} & a_{22} & a_{23} & a_{17} & a_{15} & a_{23} & a_{24} & a_{18} & a_6 & a_{17} & a_{18} & a_8 \\
a_6 & a_{15} & a_{14} & a_5 & a_{17} & a_{23} & a_{22} & a_{14} & a_{18} & a_{24} & a_{23} & a_{15} & a_8 & a_{18} & a_{17} & a_6 \\
a_7 & a_{16} & a_{13} & a_2 & a_{20} & a_{17} & a_{14} & a_{11} & a_{21} & a_{18} & a_{15} & a_{12} & a_9 & a_{19} & a_{16} & a_3 \\
a_3 & a_{16} & a_{19} & a_9 & a_{12} & a_{15} & a_{18} & a_{21} & a_{11} & a_{14} & a_{17} & a_{20} & a_2 & a_{13} & a_{16} & a_7 \\
a_6 & a_{17} & a_{18} & a_8 & a_{15} & a_{23} & a_{24} & a_{18} & a_{14} & a_{22} & a_{23} & a_{17} & a_5 & a_{14} & a_{15} & a_6 \\
a_8 & a_{18} & a_{17} & a_6 & a_{18} & a_{24} & a_{23} & a_{15} & a_{17} & a_{23} & a_{22} & a_{14} & a_6 & a_{15} & a_{14} & a_5 \\
a_9 & a_{19} & a_{16} & a_3 & a_{21} & a_{18} & a_{15} & a_{12} & a_{20} & a_{17} & a_{14} & a_{11} & a_7 & a_{16} & a_{13} & a_2 \\
a_4 & a_7 & a_9 & a_{10} & a_3 & a_6 & a_8 & a_9 & a_2 & a_5 & a_6 & a_7 & a_1 & a_2 & a_3 & a_4 \\
a_7 & a_{20} & a_{21} & a_9 & a_{16} & a_{17} & a_{18} & a_{19} & a_{13} & a_{14} & a_{15} & a_{16} & a_2 & a_{11} & a_{12} & a_3 \\
a_9 & a_{21} & a_{20} & a_7 & a_{19} & a_{18} & a_{17} & a_{16} & a_{16} & a_{15} & a_{14} & a_{13} & a_3 & a_{12} & a_{11} & a_2 \\
a_{10} & a_9 & a_7 & a_4 & a_9 & a_8 & a_6 & a_3 & a_7 & a_6 & a_5 & a_2 & a_4 & a_3 & a_2 & a_1
\end{bmatrix} \tag{18}$$

3.4. Symmetry adapted flexibility matrices and associated formulation

3.4.1. Concept of a symmetry-adapted flexibility matrix

For the treatment in this section, let us consider any subspace of dimension r, that is, the subspace is spanned by r independent basis vectors. (Notice that r has the same meaning as the n_i of Section 3.1, where in that earlier discussion, the subscript i was used to denote the number of the subspace.) We define the *symmetry-adapted flexibility coefficient* $b_{i,j}$ $(i = 1, 2, ..., r;\ j = 1, 2, ..., r)$ as the vertical deflection ensuing at *any one* of the nodes of the basis vector Φ_i as a result of unit vertical forces applied simultaneously at *all the nodes* of the basis vector Φ_j. The collection of all such coefficients constitutes the *symmetry-adapted flexibility matrix B* for that subspace.

For the 16-node structural configuration of Fig. 2(a), and as already established in Section 3.2, use of symmetry group C_{2v} results in four independent subspaces of dimensions $r = \{4, 4, 4, 4\}$, implying that the B matrix is a 4×4 matrix for all the subspaces. Use of symmetry group C_{4v} results in six independent subspaces of dimensions $r = \{3, 1, 1, 3, 4, 4\}$, so the size of the B matrix will vary from subspace to subspace, being a 3×3 matrix for Subspaces $S^{(1)}$ and $S^{(4)}$, a 1×1 matrix for Subspaces $S^{(2)}$ and $S^{(3)}$, and a 4×4 matrix for Subspaces $S^{(5A)}$ and $S^{(5B)}$.

3.4.2. Symmetry-adapted flexibility formulation based on group C_{2v}

Since $r = 4$ for all four subspaces $S^{(1)}$, $S^{(2)}$, $S^{(3)}$ and $S^{(4)}$, the symmetry-adapted flexibility matrix for all four subspaces takes the form

$$B = \begin{bmatrix} b_{1,1} & b_{1,2} & b_{1,3} & b_{1,4} \\ b_{2,1} & b_{2,2} & b_{2,3} & b_{2,4} \\ b_{3,1} & b_{3,2} & b_{3,3} & b_{3,4} \\ b_{4,1} & b_{4,2} & b_{4,3} & b_{4,4} \end{bmatrix} \tag{19}$$

Considering one subspace at a time, the coefficients of B are obtained by superimposing the appropriate values of the conventional flexibility coefficients appearing in Eq. (18), in accordance with the combinations of unit vertical forces of Φ_j plotted in Fig. 3, and taking into account the correct sign of the deflection components (a unit vertical force shown acting downwards causes *positive* displacements; a unit vertical force shown acting upwards causes *negative* displacements). Noting that the matrix B is sym-

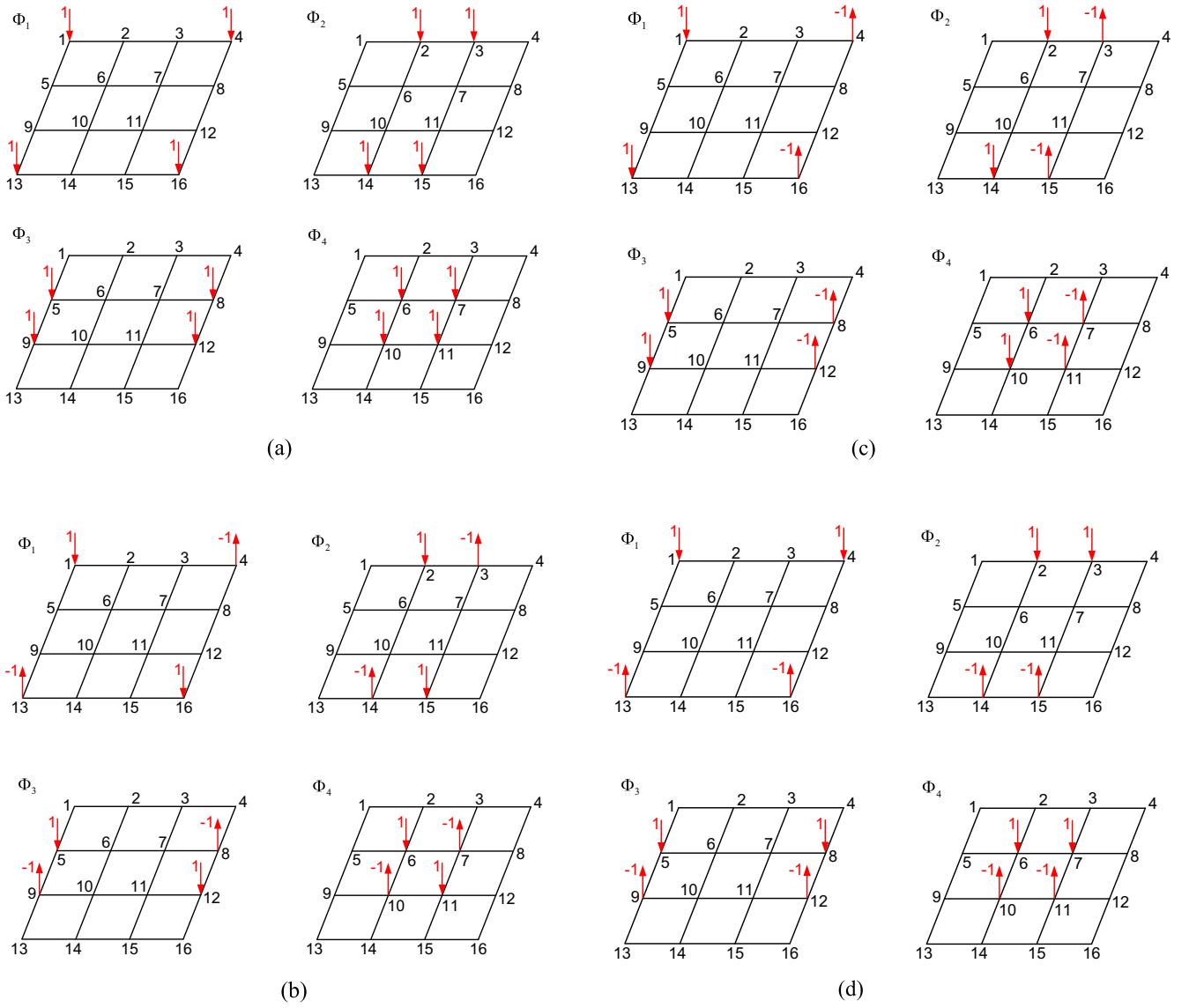

Fig. 3. Vibration analysis of the 16-node dynamic system based on the symmetry group C_{2v}: Unit vertical forces applied in accordance with the coordinates of the basis vectors: (a) subspace $S^{(1)}$; (b) subspace $S^{(2)}$; (c) subspace $S^{(3)}$; (d) subspace $S^{(4)}$.

metric ($b_{i,j} = b_{j,i}$), the distinct values of the coefficients of the B matrix are obtained as follows (the four terms on the right-hand side represent the deflections at the point in question caused by each of the four unit loads depicted in the Φ_j sets of Fig. 3):

Subspace $S^{(1)}$

$$b_{1,1} = a_1 + a_4 + a_4 + a_{10} \tag{20a}$$

$$b_{1,2} = a_2 + a_3 + a_7 + a_9 \tag{20b}$$

$$b_{1,3} = a_2 + a_7 + a_3 + a_9 \tag{20c}$$

$$b_{1,4} = a_5 + a_6 + a_6 + a_8 \tag{20d}$$

$$b_{2,2} = a_{11} + a_{12} + a_{20} + a_{21} \tag{20e}$$

$$b_{2,3} = a_{13} + a_{16} + a_{16} + a_{19} \tag{20f}$$

$$b_{2,4} = a_{14} + a_{15} + a_{17} + a_{18} \tag{20g}$$

$$b_{3,3} = a_{11} + a_{20} + a_{12} + a_{21} \tag{20h}$$

$$b_{3,4} = a_{14} + a_{17} + a_{15} + a_{18} \tag{20i}$$

$$b_{4,4} = a_{22} + a_{23} + a_{23} + a_{24} \tag{20j}$$

Subspace $S^{(2)}$

$$b_{1,1} = a_1 - a_4 - a_4 + a_{10} \tag{21a}$$

$$b_{1,2} = a_2 - a_3 - a_7 + a_9 \tag{21b}$$

$$b_{1,3} = a_2 - a_7 - a_3 + a_9 \tag{21c}$$

$$b_{1,4} = a_5 - a_6 - a_6 + a_8 \tag{21d}$$

$$b_{2,2} = a_{11} - a_{12} - a_{20} + a_{21} \tag{21e}$$

$$b_{2,3} = a_{13} - a_{16} - a_{16} + a_{19} \tag{21f}$$

$$b_{2,4} = a_{14} - a_{15} - a_{17} + a_{18} \tag{21g}$$

$$b_{3,3} = a_{11} - a_{20} - a_{12} + a_{21} \tag{21h}$$

$$b_{3,4} = a_{14} - a_{17} - a_{15} + a_{18} \tag{21i}$$

$$b_{4,4} = a_{22} - a_{23} - a_{23} + a_{24} \tag{21j}$$

Subspace $S^{(3)}$

$$b_{1,1} = a_1 - a_4 + a_4 - a_{10} \tag{22a}$$

$$b_{1,2} = a_2 - a_3 + a_7 - a_9 \tag{22b}$$

$$b_{1,3} = a_2 - a_7 + a_3 - a_9 \tag{22c}$$

$$b_{1,4} = a_5 - a_6 + a_6 - a_8 \tag{22d}$$

$$b_{2,2} = a_{11} - a_{12} + a_{20} - a_{21} \tag{22e}$$

$$b_{2,3} = a_{13} - a_{16} + a_{16} - a_{19} \tag{22f}$$

$$b_{2,4} = a_{14} - a_{15} + a_{17} - a_{18} \tag{22g}$$

$$b_{3,3} = a_{11} - a_{20} + a_{12} - a_{21} \tag{22h}$$

$$b_{3,4} = a_{14} - a_{17} + a_{15} - a_{18} \tag{22i}$$

$$b_{4,4} = a_{22} - a_{23} + a_{23} - a_{24} \tag{22j}$$

Subspace $S^{(4)}$

$$b_{1,1} = a_1 + a_4 - a_4 - a_{10} \tag{23a}$$

$$b_{1,2} = a_2 + a_3 - a_7 - a_9 \tag{23b}$$

$$b_{1,3} = a_2 + a_7 - a_3 - a_9 \tag{23c}$$

$$b_{1,4} = a_5 + a_6 - a_6 - a_8 \tag{23d}$$

$$b_{2,2} = a_{11} + a_{12} - a_{20} - a_{21} \tag{23e}$$

$$b_{2,3} = a_{13} + a_{16} - a_{16} - a_{19} \tag{23f}$$

$$b_{2,4} = a_{14} + a_{15} - a_{17} - a_{18} \tag{23g}$$

$$b_{3,3} = a_{11} + a_{20} - a_{12} - a_{21} \tag{23h}$$

$$b_{3,4} = a_{14} + a_{17} - a_{15} - a_{18} \tag{23i}$$

$$b_{4,4} = a_{22} + a_{23} - a_{23} - a_{24} \tag{23j}$$

From the above, we may make a couple of significant observations. First, if we compare the sets of expressions for the four subspaces, it is observed that corresponding $b_{i,j}$ expressions across the subspaces feature the same combination of a terms, differing only in the *signs* of the terms. Secondly, the pattern of the signs of the a terms is uniform within a given subspace, and is consistent with the symmetry of that subspace. It means that, in practical computations, the $b_{i,j}$ expressions for subspaces $S^{(2)}$, $S^{(3)}$ and $S^{(4)}$ need not be independently derived; they can simply be deduced directly from the results for subspace $S^{(1)}$ once the latter have been obtained.

The diagonal mass matrix M for a given subspace consists of non-zero diagonal elements $m_{i,i}$ (i = 1,2,...,r), which are the values of the mass at each of the nodes of the basis vector Φ_i. By reference to Fig. 3 in conjunction with Fig. 2(b), it is noted that all four subspaces have the same diagonal mass matrix, namely

$$M = \begin{bmatrix} m_1 & 0 & 0 & 0 \\ 0 & m_2 & 0 & 0 \\ 0 & 0 & m_2 & 0 \\ 0 & 0 & 0 & m_3 \end{bmatrix} \tag{24}$$

For each subspace, the eigenvalues are obtained from the vanishing condition

$$|B - \lambda M^{-1}| = 0 \tag{25}$$

where $\lambda = 1/\omega^2$, and ω is a natural circular frequency of the system. Substituting the coefficients of B (as given in generalised form by Eq. (19)) and the coefficients of M (as given by Eq. (24)) into Eq. (25), we obtain

$$\begin{vmatrix} (b_{1,1} - (\lambda/m_1)) & b_{1,2} & b_{1,3} & b_{1,4} \\ b_{2,1} & (b_{2,2} - (\lambda/m_2)) & b_{2,3} & b_{2,4} \\ b_{3,1} & b_{3,2} & (b_{3,3} - (\lambda/m_2)) & b_{3,4} \\ b_{4,1} & b_{4,2} & b_{4,3} & (b_{4,4} - (\lambda/m_3)) \end{vmatrix} = 0 \tag{26}$$

This may be expanded into a 4th-degree polynomial (characteristic equation), which is then solved (using conventional techniques) for four roots (values of λ), yielding four natural frequencies of the system. While the numerical value of the M matrix will be the same for all the four subspaces, the numerical value of the B matrix will be different for each subspace, as is clear

by reference to Eqs. (20)–(23). Thus, the solution sets for the four subspaces will be different. Solving Eq. (26) for all four subspaces yields the required 16 natural frequencies of the system.

3.4.3. Symmetry-adapted flexibility formulation based on group C_{4v}

For each of the six subspaces yielded by the symmetry group C_{4v}, the coefficients of symmetry-adapted flexibility matrix B are obtained by superimposing the appropriate values of the conventional flexibility coefficients appearing in Eq. (18), in accordance with the combinations of unit vertical forces of Φ_j plotted in Fig. 4, and taking into account the correct sign of the deflection components. The results for the symmetry-adapted flexibility matrices of all the six subspaces are as follows:

Subspaces $S^{(1)}$ and $S^{(4)}$

$$B = \begin{bmatrix} b_{1,1} & b_{1,2} & b_{1,3} \\ b_{2,1} & b_{2,2} & b_{2,3} \\ b_{3,1} & b_{3,2} & b_{3,3} \end{bmatrix} \tag{27}$$

where

$$b_{1,1} = a_1 \pm a_4 + a_{10} \tag{28a}$$

$$b_{1,2} = b_{2,1} = 2a_2 \pm 2a_3 \pm 2a_7 + 2a_9 \tag{28b}$$

$$b_{1,3} = b_{3,1} = a_5 \pm 2a_6 + a_8 \tag{28c}$$

$$b_{2,2} = a_{11} \pm a_{12} + a_{13} \pm 2a_{16} + a_{19} \pm a_{20} + a_{21} \tag{28d}$$

$$b_{2,3} = b_{3,2} = a_{14} \pm a_{15} \pm a_{17} + a_{18} \tag{28e}$$

$$b_{3,3} = a_{22} \pm 2a_{23} + a_{24} \tag{28f}$$

with the upper sign of the symbols ± or ∓ referring to subspace $S^{(1)}$ and the lower sign to subspace $S^{(4)}$.

Subspaces $S^{(2)}$ and $S^{(3)}$

$$B = [b_{1,1}] \tag{29}$$

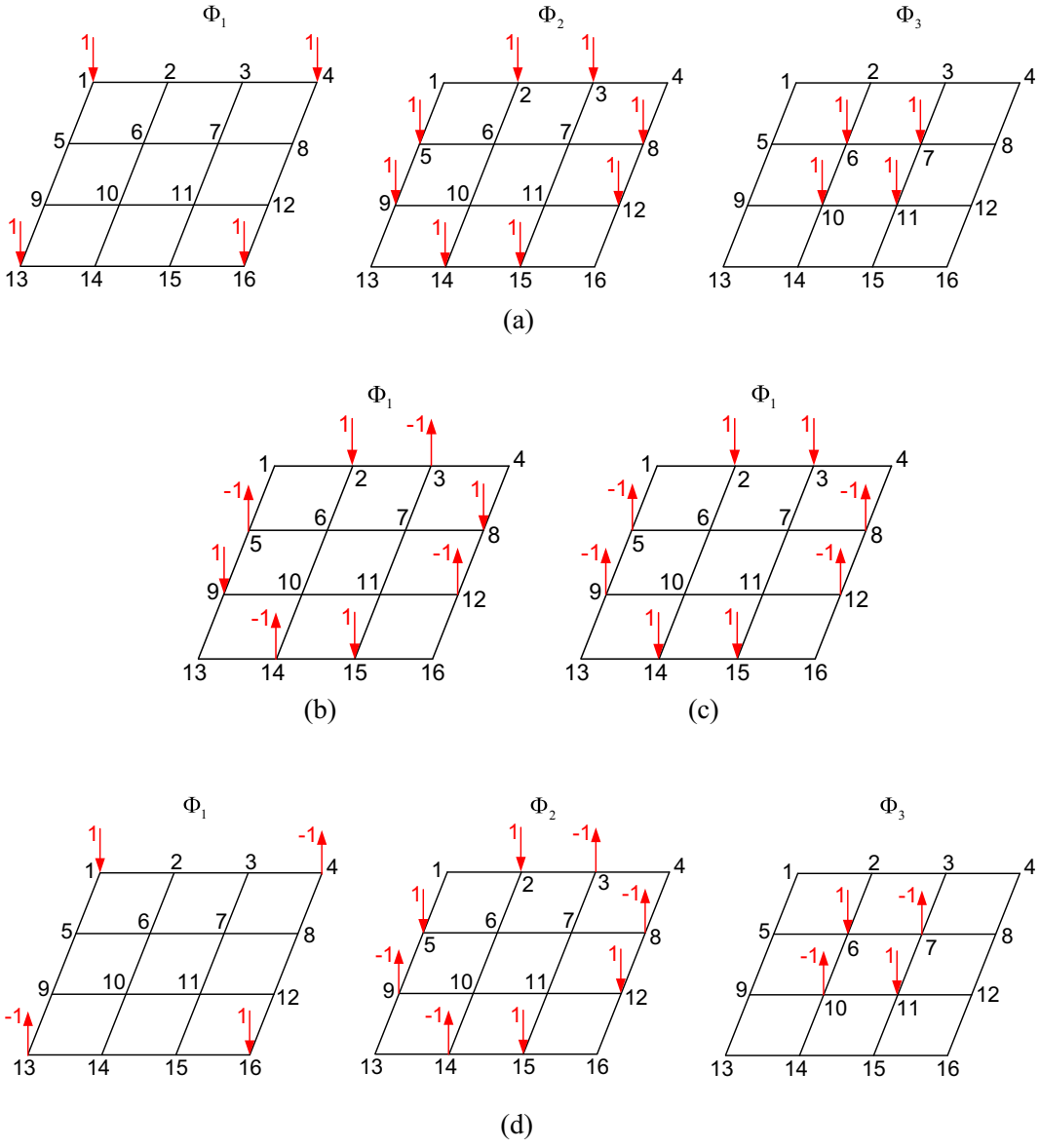

Fig. 4. Vibration analysis of the 16-node dynamic system based on the symmetry group C_{4v}: Unit vertical forces applied in accordance with the coordinates of the basis vectors: (a) subspace $S^{(1)}$; (b) subspace $S^{(2)}$; (c) subspace $S^{(3)}$; (d) subspace $S^{(4)}$; (e) subspace $S^{(5A)}$; (f) subspace $S^{(5B)}$.

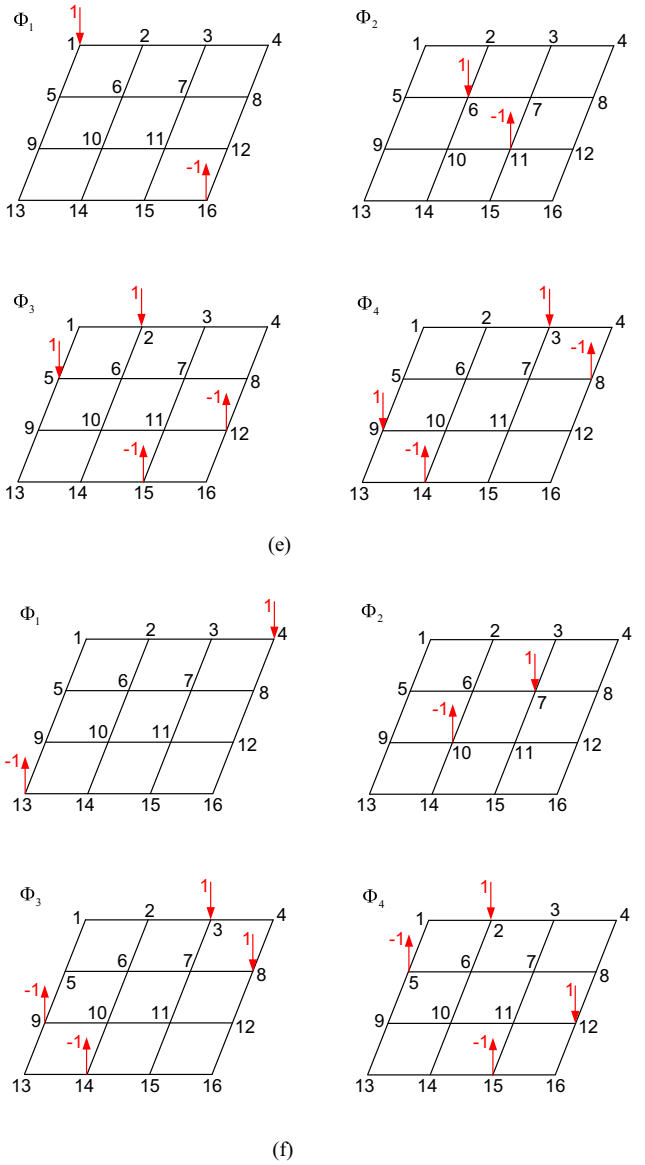

Fig. 4 (*continued*)

where

$$b_{1,\,1} = a_{11} \mp a_{12} - a_{13} \pm 2a_{16} - a_{19} \mp a_{20} + a_{21} \tag{30}$$

with the upper sign of $\pm$ or $\mp$ referring to subspace $S^{(2)}$, and the lower sign to subspace $S^{(3)}$.

Subspaces $S^{(5A)}$ and $S^{(5B)}$

$$B = \begin{bmatrix} b_{1,\,1} & b_{1,\,2} & b_{1,\,3} & b_{1,\,4} \\ b_{2,\,1} & b_{2,\,2} & b_{2,\,3} & b_{2,\,4} \\ b_{3,\,1} & b_{3,\,2} & b_{3,\,3} & b_{3,\,4} \\ b_{4,\,1} & b_{4,\,2} & b_{4,\,3} & b_{4,\,4} \end{bmatrix} \tag{31}$$

where for both subspaces,

$$b_{1,\,1} = a_1 - a_{10} \tag{32a}$$

$$b_{1,\,2} = b_{2,\,1} = a_5 - a_8 \tag{32b}$$

$$b_{1,\,3} = b_{3,\,1} = 2a_2 - 2a_9 \tag{32c}$$

$$b_{1,\,4} = b_{4,\,1} = 2a_3 - 2a_7 \tag{32d}$$

$$b_{2,\,2} = a_{22} - a_{24} \tag{32e}$$

$$b_{2,\,3} = b_{3,\,2} = 2a_{14} - 2a_{18} \tag{32f}$$

$$b_{2,\,4} = b_{4,\,2} = 2a_{15} - 2a_{17} \tag{32g}$$

$$b_{3,\,3} = a_{11} + a_{13} - a_{19} - a_{21} \tag{32h}$$

$$b_{3,\,4} = b_{4,\,3} = a_{12} - a_{20} \tag{32i}$$

$$b_{4,\,4} = a_{11} - a_{13} + a_{19} - a_{21} \tag{32j}$$

The diagonal mass matrices for the various subspaces, consisting of non-zero elements $m_{i,\,i}$ (i = 1,2,...,r), are the values of the mass at each of the nodes of the basis vector Φ_i. By reference to Fig. 4 in conjunction with Fig. 2(b), we obtain

For Subspaces $S^{(1)}$ and $S^{(4)}$

$$M = \begin{bmatrix} m_1 & 0 & 0 \\ 0 & m_2 & 0 \\ 0 & 0 & m_3 \end{bmatrix} \tag{33}$$

For Subspaces $S^{(2)}$ and $S^{(3)}$

$$M = [m_2] \tag{34}$$

For Subspaces $S^{(5A)}$ and $S^{(5B)}$

$$M = \begin{bmatrix} m_1 & 0 & 0 & 0 \\ 0 & m_3 & 0 & 0 \\ 0 & 0 & m_2 & 0 \\ 0 & 0 & 0 & m_2 \end{bmatrix} \tag{35}$$

The vanishing condition for eigenvalue determination – Eq. (25) – becomes

For Subspaces $S^{(1)}$ and $S^{(4)}$

$$\begin{vmatrix} (b_{1,\,1} - (\lambda/m_1)) & b_{1,\,2} & b_{1,\,3} \\ b_{2,\,1} & (b_{2,\,2} - (\lambda/m_2)) & b_{2,\,3} \\ b_{3,\,1} & b_{3,\,2} & (b_{3,\,3} - (\lambda/m_3)) \end{vmatrix} = 0 \tag{36}$$

using the values of $b_{i,\,j}$ (i = 1,2,3; j = 1,2,3) appropriate for each subspace, as defined by Eq. (28).

For Subspaces $S^{(2)}$ and $S^{(3)}$

$$b_{1,\,1} - (\lambda/m_2) = 0 \quad \Rightarrow \quad \lambda = b_{1,\,1}\, m_2 \tag{37}$$

using the value of $b_{1,\,1}$ appropriate for each subspace, as defined by Eq. (30).

For Subspace $S^{(5A)}$ and $S^{(5B)}$

$$\begin{vmatrix} (b_{1,\,1} - (\lambda/m_1)) & b_{1,\,2} & b_{1,\,3} & b_{1,\,4} \\ b_{2,\,1} & (b_{2,\,2} - (\lambda/m_3)) & b_{2,\,3} & b_{2,\,4} \\ b_{3,\,1} & b_{3,\,2} & (b_{3,\,3} - (\lambda/m_2)) & b_{3,\,4} \\ b_{4,\,1} & b_{4,\,2} & b_{4,\,3} & (b_{4,\,4} - (\lambda/m_2)) \end{vmatrix} = 0 \tag{38}$$

where for these two subspaces, the parameters $b_{i,\,j}$ (i = 1, 2, 3, 4; j = 1, 2, 3, 4) are identical, being given by Eq. (32) for either subspace. Subspaces $S^{(5A)}$ and $S^{(5B)}$ are a result of the decomposition of a larger subspace $S^{(5)}$ that is associated with doubly-repeating roots of λ. In problems involving the C_{4v} symmetry group, only one of subspaces $S^{(5A)}$ and $S^{(5B)}$ need to be considered in order to generate all the roots of subspace $S^{(5)}$.

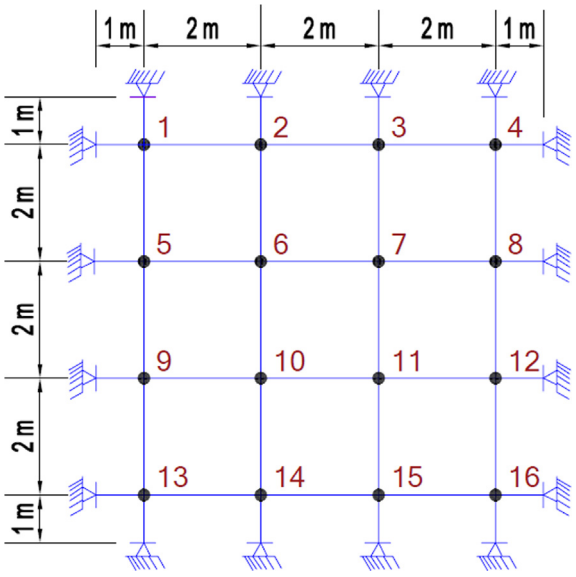

Fig. 5. Layout and dimensions of the numerical example of the 16-node plane grid.

3.5. Numerical example

Let us consider a horizontal plane grid assembled from eight aluminium beams of rectangular cross-section 0.05 m wide and 0.10 m deep. The beams are of length 8.0 m , simply supported at the ends, and spaced at 2 m in both the x and y directions, as shown in Fig. 5. The beams rigidly intersect at the 16 joints numbered as shown in the figure. The material, section and elastic properties of the grid members are as follows:

Young's modulus of elasticity: $E = 70 \times 10^6$ kN/m^2
Density of grid material: $\rho = 2700$ kg/m^3
Poisson's ratio: $\nu = 0.32$
Cross-sectional area: $A = 5 \times 10^{-3}$ m^2
Second moment of area: $I = 4.16667 \times 10^{-6}$ m^4
Flexural rigidity: $EI = 291.667$ kN m^2

We are interested in the small transverse vibrations of the grid, assuming that all the mass of the members and associated attachments is lumped at the 16 member intersections (nodes). First, we need to obtain the flexibility coefficients of the grid. The vertical (i.e. transverse) deflections at each of the 16 nodes of the grid, when a unit vertical force of 1 kN is applied at nodes 1, 2 and 6 in turn (these three locations being representative of all 16 nodes owing to symmetry), may readily be obtained from a conventional linear-elastic analysis of the grid. The results are shown in Table 1, where the values of the deflections are in millimetres (i.e. 10^{-3} m). The deflection parameters of the problem $\{a_1, a_2, \ldots, a_{24}\}$ are evaluated from the flexibility coefficients as defined by Eqs. (14)–(17), giving the results (in units of 10^{-3} m/kN):

$$a_1 = f_{1,1} = 0.97; a_2 = f_{2,1} = 0.84; a_3 = f_{3,1} = 0.38; a_4 = f_{4,1} = 0.12$$

$$a_5 = f_{6,1} = 1.35; a_6 = f_{7,1} = 0.89; a_7 = f_{8,1} = 0.29; a_8 = f_{11,1} = 0.78$$

$$a_9 = f_{12,1} = 0.29; a_{10} = f_{16,1} = 0.12; a_{11} = f_{2,2} = 2.16; a_{12} = f_{3,2} = 1.32$$

$$a_{13} = f_{5,2} = 1.35; a_{14} = f_{6,2} = 3.03; a_{15} = f_{7,2} = 2.49; a_{16} = f_{8,2} = 0.89$$

$$a_{17} = f_{10,2} = 2.05; a_{18} = f_{11,2} = 1.95; a_{19} = f_{12,2} = 0.78; a_{20} = f_{14,2} = 0.71$$

$$a_{21} = f_{15,2} = 0.71; a_{22} = f_{6,6} = 7.13; a_{23} = f_{7,6} = 5.70; a_{24} = f_{11,6} = 5.09$$

Let us illustrate the group-theoretic computational steps by applying symmetry group C_{2v} to our numerical example. The symmetry-adapted flexibility matrix for each of the four subspaces of the problem takes the form given by Eq. (19), where the symmetry-adapted flexibility coefficients $b_{i,j}$ ($i = 1, 2, 3, 4$; $j = 1, 2, 3, 4$) for each subspace are linear combinations of the deflection parameters as given by Eqs. (20)–(23). Evaluating the $b_{i,j}$ for all four subspaces of the problem, we obtain the following results for the symmetry-adapted flexibility matrices $B^{(1)}$, $B^{(2)}$, $B^{(3)}$ and $B^{(4)}$ for subspaces $S^{(1)}$, $S^{(2)}$, $S^{(3)}$ and $S^{(4)}$ respectively, with the units of the flexibility coefficients being 10^{-3} m/kN:

$$B^{(1)} = \begin{bmatrix} 1.33 & 1.80 & 1.80 & 3.91 \\ 1.80 & 4.90 & 3.91 & 9.52 \\ 1.80 & 3.91 & 4.90 & 9.52 \\ 3.91 & 9.52 & 9.52 & 23.62 \end{bmatrix}; B^{(2)} = \begin{bmatrix} 0.85 & 0.46 & 0.46 & 0.35 \\ 0.46 & 0.84 & 0.35 & 0.44 \\ 0.46 & 0.35 & 0.84 & 0.44 \\ 0.35 & 0.44 & 0.44 & 0.82 \end{bmatrix}$$

$$B^{(3)} = \begin{bmatrix} 0.85 & 0.46 & 0.64 & 0.57 \\ 0.46 & 0.84 & 0.57 & 0.64 \\ 0.64 & 0.57 & 2.06 & 1.52 \\ 0.57 & 0.64 & 1.52 & 2.04 \end{bmatrix}; B^{(4)} = \begin{bmatrix} 0.85 & 0.64 & 0.46 & 0.57 \\ 0.64 & 2.06 & 0.57 & 1.52 \\ 0.46 & 0.57 & 0.84 & 0.64 \\ 0.57 & 1.52 & 0.64 & 2.04 \end{bmatrix}$$

Let us assume all the mass of the dynamic system stems only from the mass of the grid members, which we will lump at the nodes of the grid. From the layout in Fig. 5, a grid spacing of 2 m implies that 4 m of member length is supported by each node. The concentrated mass m_n at each node ($n = 1, 2, \ldots, 16$), given that the member cross-sectional area is 0.005 m^2 and the density of aluminium is 2700 kg/m^3, is therefore 54kg. Each of the four subspaces of the problem has the same diagonal mass matrix given by Equation (24). In the present example, all nodal masses have a value of 54kg, so the mass matrix for each subspace $S^{(i)}$ ($i = 1, 2, 3, 4$) is given by

$$M^{(i)} = \begin{bmatrix} 54 & 0 & 0 & 0 \\ 0 & 54 & 0 & 0 \\ 0 & 0 & 54 & 0 \\ 0 & 0 & 0 & 54 \end{bmatrix}$$

with the units of the diagonal elements being kilograms. Eigenvalues for each subspace are evaluated on the basis of Eq. (26), using the $b_{i,j}$

Table 1
Vertical deflections (in millimetres) at the 16 nodes of the grid due to a unit vertical load of 1 kN applied at node 1, at node 2 and at node 6 (one unit load at a time).

		Node at which unit load is applied		
		1	**2**	**6**
Node at which vertical deflection is measured	**1**	0.97	0.84	1.35
	2	0.84	2.16	3.03
	3	0.38	1.32	2.49
	4	0.12	0.38	0.89
	5	0.84	1.35	3.03
	6	1.35	3.03	7.13
	7	0.89	2.49	5.7
	8	0.29	0.89	2.05
	9	0.38	0.89	2.49
	10	0.89	2.05	5.7
	11	0.78	1.95	5.09
	12	0.29	0.78	1.95
	13	0.12	0.29	0.89
	14	0.29	0.71	2.05
	15	0.29	0.71	1.95
	16	0.12	0.29	0.78

values ($i = 1, 2, 3, 4$; $j = 1, 2, 3, 4$) for the subspace in question, and the $m_{i,i}$ values ($i = 1, 2, 3, 4$) of 54 kg. The eigenvectors Ψ for each subspace then follow from the subspace eigenvalue equation

$$\left[\left[B^{(i)}\right] - \lambda\left[M^{(i)}\right]^{-1}\right]\{\Psi\} = \{0\} \tag{39}$$

The results for eigenvalues λ, natural frequencies of vibration $f\ (= 1/\{2\pi\lambda^{0.5}\})$ and eigenvectors Ψ, obtained for each subspace, are as follows:

Subspaces $S^{(1)}$

$\lambda_1 = 1.7432 \quad \lambda_2 = 0.02760 \quad \lambda_3 = 0.05219 \quad \lambda_4 = 0.05346$

$f_1 = 0.121$ Hz $\quad f_2 = 0.958$ Hz $\quad f_3 = 0.697$ Hz $\quad f_4 = 0.688$ Hz

$$\Psi_1 = \begin{Bmatrix} 0.175 \\ 0.418 \\ 0.418 \\ 1.000 \end{Bmatrix} \quad \Psi_2 = \begin{Bmatrix} 1.000 \\ -0.415 \\ -0.415 \\ 0.174 \end{Bmatrix} \quad \Psi_3 = \begin{Bmatrix} -0.994 \\ -0.986 \\ -0.986 \\ 1.000 \end{Bmatrix}$$

$$\Psi_4 = \begin{Bmatrix} 0.000 \\ -1.000 \\ 1.000 \\ 0.000 \end{Bmatrix}$$

Subspaces $S^{(2)}$

$\lambda_1 = 0.1127 \quad \lambda_2 = 0.01552 \quad \lambda_3 = 0.02617 \quad \lambda_4 = 0.02646$

$f_1 = 0.474$ Hz $\quad f_2 = 1.278$ Hz $\quad f_3 = 0.984$ Hz $\quad f_4 = 0.978$ Hz

$$\Psi_1 = \begin{Bmatrix} 1.000 \\ 0.982 \\ 0.982 \\ 0.957 \end{Bmatrix} \quad \Psi_2 = \begin{Bmatrix} 1.000 \\ -0.973 \\ -0.973 \\ 0.951 \end{Bmatrix} \quad \Psi_3 = \begin{Bmatrix} -0.953 \\ -0.001 \\ -0.001 \\ 1.000 \end{Bmatrix}$$

$$\Psi_4 = \begin{Bmatrix} 0.000 \\ -1.000 \\ 1.000 \\ 0.000 \end{Bmatrix}$$

Subspaces $S^{(3)}$

$\lambda_1 = 0.2211 \quad \lambda_2 = 0.04214 \quad \lambda_3 = 0.01926 \quad \lambda_4 = 0.03014$

$f_1 = 0.338$ Hz $\quad f_2 = 0.775$ Hz $\quad f_3 = 1.147$ Hz $\quad f_4 = 0.917$ Hz

$$\Psi_1 = \begin{Bmatrix} 0.433 \\ 0.432 \\ 1.000 \\ 0.994 \end{Bmatrix} \quad \Psi_2 = \begin{Bmatrix} 1.000 \\ 0.980 \\ -0.444 \\ -0.415 \end{Bmatrix} \quad \Psi_3 = \begin{Bmatrix} -0.974 \\ 1.000 \\ 0.393 \\ -0.405 \end{Bmatrix}$$

$$\Psi_4 = \begin{Bmatrix} -0.409 \\ 0.394 \\ -0.986 \\ 1.000 \end{Bmatrix}$$

Subspaces $S^{(4)}$

$\lambda_1 = 0.2211 \quad \lambda_2 = 0.04214 \quad \lambda_3 = 0.01926 \quad \lambda_4 = 0.03014$

$f_1 = 0.338$ Hz $\quad f_2 = 0.775$ Hz $\quad f_3 = 1.147$ Hz $\quad f_4 = 0.917$ Hz

$$\Psi_1 = \begin{Bmatrix} 0.433 \\ 1.000 \\ 0.432 \\ 0.994 \end{Bmatrix} \quad \Psi_2 = \begin{Bmatrix} 1.000 \\ -0.444 \\ 0.980 \\ -0.415 \end{Bmatrix} \quad \Psi_3 = \begin{Bmatrix} -0.974 \\ 0.393 \\ 1.000 \\ -0.405 \end{Bmatrix}$$

$$\Psi_4 = \begin{Bmatrix} -0.409 \\ -0.986 \\ 0.394 \\ 1.000 \end{Bmatrix}$$

The subspace eigenvalues and natural frequencies are also the eigenvalues and natural frequencies of the original problem. A formal proof of this may be seen in older literature on applications of group theory to physical problems [1]. However, subspace eigenvectors are only eigenvectors in the 4-dimensional space of the subspace in question. To convert these to eigenvectors in the 16-dimensional vector space of the original problem, we allocate the calculated ordinate of the subspace eigenvector *to all the grid notes of the associated basis vector* (see Eqs. (4)–(7)), with the signs (positive or negative) of the allocations being in accordance with the signs of the basis-vector terms.

As an example, consider the first eigenvector Ψ_1 of subspace $S^{(1)}$. We want to convert this into an eigenvector in the full space of the original problem. We note that the ordinates of Ψ_1 are $\{0.175;\ 0.418;\ 0.418;\ 1.000\}$. Looking at Eq. (4), we see that there are four basis vectors $\Phi_1^{(1)}$, $\Phi_2^{(1)}$, $\Phi_3^{(1)}$ and $\Phi_4^{(1)}$ spanning the subspace $S^{(1)}$, and these are associated with the grid nodal sets $\{1, 16, 13, 4\}$, $\{2, 15, 14, 3\}$, $\{5, 12, 9, 8\}$ and $\{6, 11, 10, 7\}$ respectively, given by the numerical subscripts of the w_i. Eigenvalues in the full vector space of the original problem are obtained by allocating the value $+0.175$ to nodes $\{1, 16, 13, 4\}$, the value $+0.418$ to nodes $\{2, 15, 14, 3\}$, the value $+0.418$ to nodes $\{5, 12, 9, 8\}$, and the value $+1.000$ to nodes $\{6, 11, 10, 7\}$, the value for each node i being the ordinate of Ψ_1 multiplied by the sign of the associated w_i (i.e. multiplied by $+1$, since all the w_i in Eq. (4) have positive signs).

The values allocated in the above manner are the relative displacement ordinates U_1 of the 16 nodes of the grid which, when viewed together, give the mode shape corresponding to the first eigenvector Ψ_1 of subspace $S^{(1)}$. Written as a column vector, U_1 is therefore 16-dimensional. Allocating Ψ_2, Ψ_3 and Ψ_4 in the same manner generates modes U_2, U_3 and U_4 of subspace $S^{(1)}$. Thus, each of the four subspaces yields four modes of vibration $\{U_1, U_2, U_3, U_4\}$, and the four subspaces taken together yield the 16 modes of vibration of the grid. The full sets of results (i.e. relative displacement ordinates) for all 16 modes of vibration of the grid are shown in Table 2, and plotted as Figs. 6–9. From the plots, it is clear that modes belonging to the same subspace have the same patterns (i.e. symmetry type), and these patterns differ from one subspace to another.

The results for the frequencies clearly show that subspaces $S^{(2)}$ and $S^{(3)}$ yield identical sets of frequencies, whereas the sets of frequencies for subspaces $S^{(1)}$ and $S^{(4)}$ are different from each other and from those of sets $S^{(2)}$ and $S^{(3)}$. Thus, the grid has 4 doubly-occurring and 8 singly-occurring frequencies, giving 12 distinct frequencies in total. Here, another computational merit of group-theoretic decomposition becomes evident. By computing the frequencies in separate subspaces, the group-theoretic approach bypasses the numerical problems usually associated with solving for roots (eigenvalues) that coincide with each other, or that are too close to each other.

It should be noted that the point of group-theoretic calculations is not to obtain greater accuracy; rather, it is about simplifying computations through subspace decomposition; group theory also allows us to gain insights on physical behaviour that is peculiar to symmetric structures. In itself, group-theoretic decomposition is a mathematically exact process, therefore as long as the basic structural theory is correct, the results of group-theoretic simplifications will also be correct.

As already seen in Section 3.2, if symmetry group C_{4v} had been used, the two subspaces with identical roots would be known right from the outset, necessitating the consideration of only one of these to yield the 4 doubly-occurring frequencies. For this problem, the symmetry group C_{4v} would be the better one to use from a

Table 2
Relative displacement ordinates of the 16 nodes of the grid, defining the 16 modes of vibration of the grid. Each symmetry subspace is associated with four modes of vibration $\{U_1, U_2, U_3, U_4\}$.

Node	Subspace $S^{(1)}$				Subspace $S^{(2)}$				Subspace $S^{(3)}$				Subspace $S^{(4)}$			
	U_1	U_2	U_3	U_4	U_1	U_2	U_3	U_4	U_1	U_2	U_3	U_4	U_1	U_2	U_3	U_4
1	0.175	1.000	−0.994	0.000	1.000	1.000	−0.953	0.000	0.433	1.000	−0.974	−0.409	0.433	1.000	−0.974	−0.409
2	0.418	−0.415	−0.986	−1.000	0.982	−0.973	−0.001	−1.000	0.432	0.980	1.000	0.394	1.000	−0.444	0.393	−0.986
3	0.418	−0.415	−0.986	−1.000	−0.982	0.973	0.001	1.000	−0.432	−0.980	−1.000	−0.394	1.000	−0.444	0.393	−0.986
4	0.175	1.000	−0.994	0.000	−1.000	−1.000	0.953	0.000	−0.433	−1.000	0.974	0.409	0.433	1.000	−0.974	−0.409
5	0.418	−0.415	−0.986	1.000	0.982	−0.973	−0.001	1.000	1.000	−0.444	0.393	−0.986	0.432	0.980	1.000	0.394
6	1.000	0.174	1.000	0.000	0.957	0.951	1.000	0.000	0.994	−0.415	−0.405	1.000	0.994	−0.415	−0.405	1.000
7	1.000	0.174	1.000	0.000	−0.957	−0.951	−1.000	0.000	−0.994	0.415	0.405	−1.000	0.994	−0.415	−0.405	1.000
8	0.418	−0.415	−0.986	1.000	−0.982	0.973	0.001	−1.000	−1.000	0.444	−0.393	0.986	0.432	0.980	1.000	0.394
9	0.418	−0.415	−0.986	1.000	−0.982	0.973	0.001	−1.000	1.000	−0.444	0.393	−0.986	−0.432	−0.980	−1.000	−0.394
10	1.000	0.174	1.000	0.000	−0.957	−0.951	−1.000	0.000	0.994	−0.415	−0.405	1.000	−0.994	0.415	0.405	−1.000
11	1.000	0.174	1.000	0.000	0.957	0.951	1.000	0.000	−0.994	0.415	0.405	−1.000	−0.994	0.415	0.405	−1.000
12	0.418	−0.415	−0.986	1.000	0.982	−0.973	−0.001	1.000	−1.000	0.444	−0.393	0.986	−0.432	−0.980	−1.000	−0.394
13	0.175	1.000	−0.994	0.000	−1.000	−1.000	0.953	0.000	0.433	1.000	−0.974	−0.409	−0.433	−1.000	0.974	0.409
14	0.418	−0.415	−0.986	−1.000	−0.982	0.973	0.001	1.000	0.432	0.980	1.000	0.394	−1.000	0.444	−0.393	0.986
15	0.418	−0.415	−0.986	−1.000	0.982	−0.973	−0.001	−1.000	−0.432	−0.980	−1.000	−0.394	−1.000	0.444	−0.393	0.986
16	0.175	1.000	−0.994	0.000	1.000	1.000	−0.953	0.000	−0.433	−1.000	0.974	0.409	−0.433	−1.000	0.974	0.409

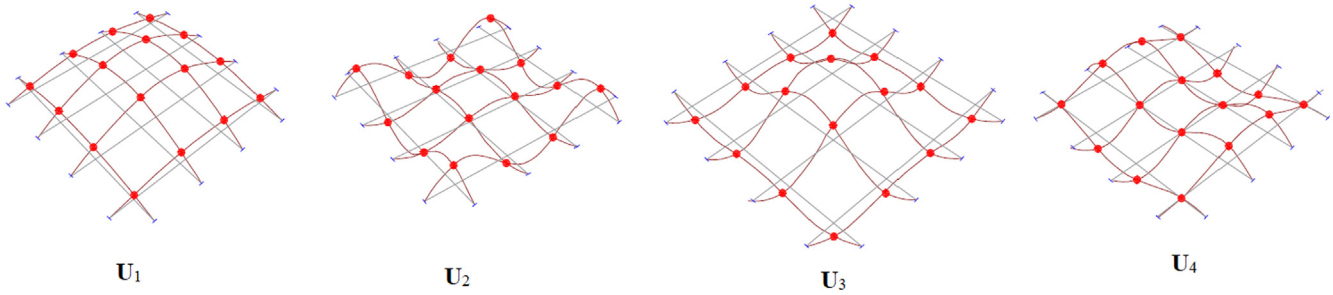

Fig. 6. Modes associated with subspace $S^{(1)}$ of the numerical example of the 16-node plane grid, derived on the basis of symmetry group C_{2v}.

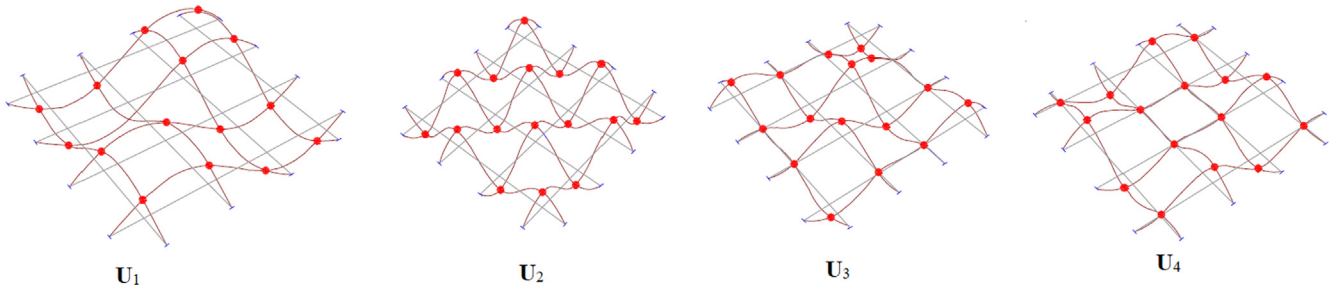

Fig. 7. Modes associated with subspace $S^{(2)}$ of the numerical example of the 16-node plane grid, derived on the basis of symmetry group C_{2v}.

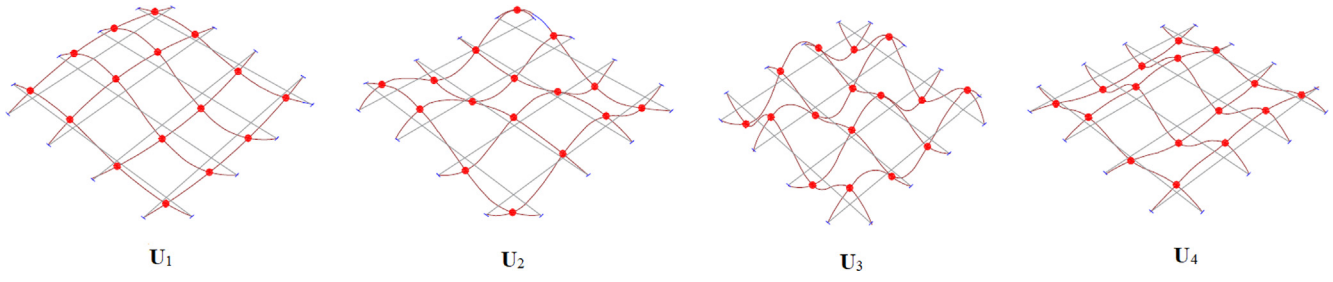

Fig. 8. Modes associated with subspace $S^{(3)}$ of the numerical example of the 16-node plane grid, derived on the basis of symmetry group C_{2v}.

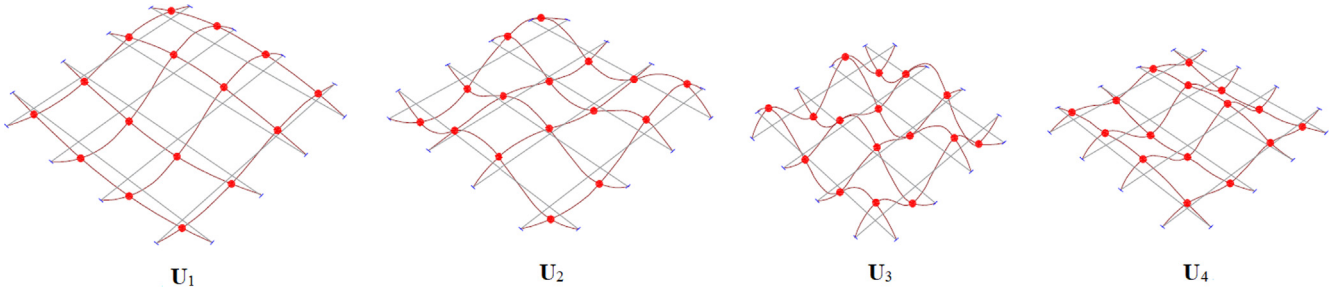

Fig. 9. Modes associated with subspace $S^{(4)}$ of the numerical example of the 16-node plane grid, derived on the basis of symmetry group C_{2v}.

computational viewpoint (but see the comments in the next section).

3.6. Final remarks on the 16-node dynamic system

We have seen how use of group C_{2v} decomposes the vector space of the configuration of Fig. 2(a) (which is of dimension $n = 16$) into four subspaces of dimensions $n_i = \{4, 4, 4, 4\}$. On the other hand, use of group C_{4v} has decomposed the problem into six subspaces of dimensions $n_i = \{3, 1, 1, 3, 4, 4\}$. The eigenvalue problem has been formulated on the basis of these two symmetry groups, and the computational merits of each clearly illustrated by setting up the equations for the extraction of all 16 eigenvalues (i.e. natural frequencies of vibration) of the system.

As remarked earlier, the decomposition achieved by the use of group C_{4v} is of higher degree than that achieved by the use of group C_{2v}, but the more uniform decomposition afforded by group C_{2v} may make it a better choice for large-scale problems where it is desired to split the computations evenly across a number of parallel processors. However, there are also other factors to take into account. In the next section, we will extend the discussion to other symmetry groups, and propose a quantitative criterion for the selection of the most optimal symmetry group.

4. Criterion for best choice of symmetry group

Now the total computational effort involved in obtaining the solutions (matrix multiplications, evaluation of determinants, finding the roots of polynomial equations, numerical integrations, etc.) may be taken as generally proportional to n^3, where n is the dimension (or the total number of unknowns) of the full space of the problem. A measure of the computational benefit of group-theoretic decomposition is thus given by the ratio $\sum n_i^3/n^3$, where n_i $(i = 1, 2, \ldots, k)$ is the dimension of subspace $S^{(i)}$ of the problem, and k is the number of independent subspaces yielded by the use of a particular symmetry group. Given a number of possible symmetry groups (such as O_h, O, D_{4h}, D_{2h}, C_{4v}, C_{2v} and C_{1v} in the case of a cubic configuration), the most appropriate symmetry group is that which results in the smallest value of the ratio $\sum n_i^3/n^3$.

Let us apply this criterion to the 16-node example of Section 3 (where $n = 16$), for which group C_{2v} decomposed the vector space of the problem into four subspaces of dimensions $n_i = \{4, 4, 4, 4\}$ while group C_{4v} decomposed the problem into six subspaces of dimensions $n_i = \{3, 1, 1, 3, 4, 4\}$. Noting that only one of the 4-dimensional subspaces of group C_{4v} needs to be considered in an analysis (since the two 4-dimensional subspaces yield identical solutions), we obtain for the computational ratio $(\sum n_i^3)/n^3$:

$$C_{2v}: \frac{1}{16^3}\left(4^3 + 4^3 + 4^3 + 4^3\right) = \frac{256}{4096} = 0.0625$$

$$C_{4v}: \frac{1}{16^3}\left(3^3 + 1^3 + 1^3 + 3^3 + 4^3\right) = \frac{120}{4096} = 0.0293$$

For this example of a system with C_{4v} symmetry and 16 degrees of freedom, use of the symmetry group C_{4v}, with the smaller ratio of 0.0293, is therefore more computationally efficient than use of its subgroup C_{2v}. If advantage had not been taken of the identical nature of the two 4-dimensional subspaces of group C_{4v}, the computational ratio for group C_{4v} would have been

$$C_{4v}: \frac{1}{16^3}\left(3^3 + 1^3 + 1^3 + 3^3 + 4^3 + 4^3\right) = \frac{184}{4096} = 0.0449$$

The group C_{4v} would still remain the more computationally efficient.

5. Application to the octahedral group O_h

Let us focus attention on the cubic configuration of Fig. 1(d), whose eight nodes and associated sets of nodal vectors conform to the symmetry group O_h. The basis vectors of the subspaces of symmetry groups O_h, O, D_{4h}, D_{2h}, C_{4v}, C_{2v} and C_{1v} are obtained following the procedure explained in Section 3, by applying the idempotents of these symmetry groups upon nodal vector sets $\psi_1, \psi_2, \ldots, \psi_8$ associated with nodes 1, 2, ..., 8. The nodal vector sets are the sets of degrees of freedom at each node (e.g. ψ_1 may represent the three orthogonal displacements $\{u_1, v_1, w_1\}$ at Node 1). Let us consider the simple situation where a node is associated with only one degree of freedom, i.e. the displacement along the line joining the node to the centre of the cube. The dimension of the full vector space (i.e. the number of basis vectors spanning the space) of the cubic configuration is given by $n = 8$. For the symmetry group O_h and its subgroups, group-theoretic decomposition yields the dimensions n_i of the associated subspaces as follows:

Group O: 5 Subspaces: n_i $(i = 1, 2, \ldots, 5)$ = 1, 1, 0, 3, 3
Group D_{4h}: 10 Subspaces: n_i $(i = 1, 2, \ldots, 10)$ = 1, 0, 0, 1, 2(1,1), 0, 1, 1, 0, 2(1,1)
Group D_{2h}: 8 Subspaces: n_i $(i = 1, 2, \ldots, 8)$ = 1, 1, 1, 1, 1, 1, 1, 1
Group C_{4v}: 5 Subspaces: n_i $(i = 1, 2, \ldots, 5)$ = 2, 0, 0, 2, 4(2,2)
Group C_{2v}: 4 Subspaces: n_i $(i = 1, 2, 3, 4)$ = 2, 2, 2, 2
Group C_{1v}: 2 Subspaces: n_i $(i = 1, 2)$ = 4, 4

For groups D_{4h} and C_{4v}, the numbers in brackets denote degeneration of each 2-dimensional subspace into two 1-dimensional subspaces with identical solutions, and degeneration of the 4-dimensional subspace into two 2-dimensional subspaces with identical solutions, a beneficial consequence of the existence of repeating solutions in these subspaces. For these subspaces, only one of the two degenerate subspaces with identical solutions need to be considered, which reduces computational effort even further. For the null subspaces (i.e. those subspaces for which n_i is zero), no computations are required because no solutions (i.e. eigenvalues in the case of vibration problems) lie in these subspaces. In the computations below, the zero values for the null subspaces will be retained for the sake of clarity, but clearly they do not affect the results.

Applying our criterion to the above groups, and considering only one of the two degenerate subspaces with identical solutions in the case of groups D_{4h} and C_{4v}, we obtain for $(\sum n_i^3)/n^3$

$$O : \frac{1}{8^3}\left(1^3+1^3+0+3^3+3^3\right) = \frac{56}{512} = 0.1094$$

$$D_{4h} : \frac{1}{8^3}\left(1^3+0+0+1^3+1^3+0+1^3+1^3+0+1^3\right) = \frac{6}{512} = 0.0117$$

$$D_{2h} : \frac{1}{8^3}\left(1^3+1^3+1^3+1^3+1^3+1^3+1^3+1^3\right) = \frac{8}{512} = 0.0156$$

$$C_{4v} : \frac{1}{8^3}\left(2^3+0+0+2^3+2^3\right) = \frac{24}{512} = 0.0469$$

$$C_{2v} : \frac{1}{8^3}\left(2^3+2^3+2^3+2^3\right) = \frac{32}{512} = 0.0625$$

$$C_{1v} : \frac{1}{8^3}\left(4^3+4^3\right) = \frac{128}{512} = 0.2500$$

Thus, the symmetry group D_{4h}, with the lowest value (0.0117) of the ratio $\sum n_i^3/n^3$, is the most computationally efficient for this particular problem of an 8 d.o.f. cubic configuration with octahedral symmetry, followed by symmetry group D_{2h} with the computational ratio of 0.0156. It should be noted that if advantage had not been taken of the degenerate nature of one subspace of the symmetry group D_{4h}, the computational ratio for the symmetry group D_{4h} would have worked out at 0.0391, thus making the symmetry group D_{2h} the most efficient.

6. Summary and conclusions

In this paper, we have illustrated, on the basis of symmetry groups C_{2v} and C_{4v}, the procedure for determining the dimensions of the subspaces for a given physical problem, prior to performing any detailed calculations. For discrete models of dynamic systems undergoing small transverse vibrations (such as plane grids, space grids, cable nets and plates), we have presented a rigorous procedure for the derivation of subspace flexibility matrices from an arbitrary set of conventional flexibility coefficients. This procedure can easily be programmed for numerical implementation.

To illustrate the application of the method to a real vibration problem, including the computational steps involved, a numerical example of the small transverse vibrations of a 16-node plane grid has been considered, and the symmetry group C_{2v} applied to compute all 16 natural frequencies and 16 mode shapes of the system. The analysis has revealed the existence of doubly-occurring frequencies, and highlighted yet another merit of the group-theoretic method: by computing frequencies in separate and independent subspaces, the procedure bypasses the numerical problems usually associated with solving for eigenvalues that coincide with each other, or that are too close to each other.

For the widely applicable case study of the 16-node plane configuration undergoing small transverse vibrations, it has been found that the decomposition achieved by the use of group C_{4v} is of higher degree than that achieved by the use of group C_{2v}. However, the more uniform decomposition afforded by group C_{2v} may make it a better choice for large-scale problems where it is desired to split the computations as evenly as possible across a number of parallel processors.

Considerations have been extended to more general circumstances. In situations where more than one symmetry group is applicable (typically physical systems with complex symmetry), a simple criterion for the identification of the most efficient symmetry group has been proposed, and applied to the case of an 8 d.o.f. cubic configuration with octahedral symmetry. For this example, it has been shown that the group D_{4h} is the most efficient, and hence the most appropriate for computational purposes, followed by group D_{2h}. If advantage is not taken of the degenerate nature of one subspace of the group D_{4h}, the group D_{2h}, with its eight 1-dimensional subspaces, becomes the most efficient, followed by the group D_{4h}. Groups O, C_{4v}, C_{2v} and C_{1v} do not decompose the problem sufficiently, and are thus not very efficient.

In this treatment, we have chosen to illustrate the group-theoretic computational procedure by reference to problems that have a relatively small number of unknowns or degrees of freedom, to allow the reader to follow the steps more easily. It should be pointed out that these group-theoretic computational steps, as well as the criterion that has been proposed for identifying the best symmetry group, are also applicable to large-scale problems, as long as the configurations have symmetry properties that can be identified with known symmetry groups. The treatment has inherently assumed that one is already aware of the various symmetry groups that are applicable to a particular problem, and that it is just a question of deciding which one is the most applicable group to adopt in an analysis. For many configurations encountered in real engineering situations, the possible symmetry groups are clearly evident from a simple visual inspection of the symmetry properties of the configuration (number and orientation of reflection planes, rotation axes, etc.), but in the case of more complex configurations where the symmetry groups are not so obvious, more systematic procedures for identifying symmetry properties and all possible symmetry groups are available in the literature [52–55].

In general, the most efficient symmetry group for a given structural configuration depends on the number and arrangement of nodes and members, as well as the number and arrangement of degrees of freedom of the problem, including how the nodes and members are arranged with respect to the axes of symmetry and reflection planes of the configuration.

In summary, the present study has illustrated in detail the procedure for determining the dimensions of the various subspaces of a given physical problem, prior to performing any detailed calculations, as well as the steps involved in computing actual frequencies and mode shapes. Where a number of alternative symmetry groups are possible, a rational criterion for selecting the most computationally efficient symmetry group, prior to any detailed computations, has been proposed for the first time. This is the main achievement of this contribution.

References

[1] Hamermesh M. Group theory and its application to physical problems. Oxford: Pergamon Press; 1962.
[2] Weyl H. Theory of groups and quantum mechanics. New York: Dover Publications; 1932.
[3] Wigner EP. Group theory and its applications to the quantum mechanics of atomic spectra. New York: Academic Press; 1959.
[4] Schonland D. Molecular symmetry. London: Van Nostrand; 1965.
[5] Wherrett BS. Group theory for atoms, molecules and solids. Englewood Cliffs (NJ): Prentice-Hall; 1986.
[6] Chou TT, Yang CN. Exact solution of the vibration problem for the carbon-60 molecule. Phys Lett A 1997;235:97–104.
[7] Renton JD. On the stability analysis of symmetrical frameworks. Q J Mech Appl Math 1964;17:175–97.
[8] Sattinger DH. Group theoretic methods in bifurcation theory. Lecture notes in mathematics, vol. 762. Berlin: Springer; 1979.
[9] Ikeda K, Murota K. Bifurcation analysis of symmetric structures using block-diagonalisation. Comput Meth Appl Mech Eng 1991;86:215–43.
[10] Ikeda K, Murota K, Fujii H. Bifurcation hierarchy of symmetric structures. Int J Solids Struct 1991;27(12):1551–73.
[11] Healey TJ. A group-theoretic approach to computational bifurcation problems with symmetry. Comput Meth Appl Mech Eng 1988;67:257–95.

[12] Wohlever JC, Healey TJ. A group-theoretic approach to the global bifurcation analysis of an axially compressed cylindrical shell. Comput Meth Appl Mech Eng 1995;122:315–49.
[13] Glockner PG. Symmetry in structural mechanics. ASCE J Struct Divis 1973;99 (ST1):71–89.
[14] Zingoni A, Pavlovic MN, Zlokovic GM. A symmetry-adapted flexibility approach for multi-storey space frames: general outline and symmetry-adapted redundants. Struct Eng Rev 1995;7:107–19.
[15] Zingoni A, Pavlovic MN, Zlokovic GM. A symmetry-adapted flexibility approach for multi-storey space frames: symmetry-adapted loads. Struct Eng Rev 1995;7:121–30.
[16] Harth P, Michelberger P. Determination of loads in quasi-symmetric structure with symmetry components. Eng Struct 2016;123:395–407.
[17] Kangwai RD, Guest SD, Pellegrino S. An introduction to the analysis of symmetric structures. Comput Struct 1999;71:671–88.
[18] Kangwai RD, Guest SD. Detection of finite mechanisms in symmetric structures. Int J Solids Struct 1999;36:5507–27.
[19] Kangwai RD, Guest SD. Symmetry-adapted equilibrium matrices. Int J Solids Struct 2000;37:1525–48.
[20] Fowler PW, Guest SD. A symmetry extension of Maxwell's rule for rigidity of frames. Int J Solids Struct 2000;37(12):1793–804.
[21] Guest SD, Fowler PW. Symmetry conditions and finite mechanisms. J Mech Mater Struct 2007;2(2):293–301.
[22] Chen Y, Feng J. Generalized eigenvalue analysis of symmetric prestressed structures using group theory. J Comput Civil Eng 2012;26(4):488–97.
[23] Chen Y, Sareh P, Feng J. Effective insights into the geometric stability of symmetric skeletal structures under symmetric variations. Int J Solids Struct 2015;69/70:277–90.
[24] Chen Y, Feng J, Ma R, Zhang Y. Efficient symmetry method for calculating integral prestress modes of statically indeterminate cable-strut structures. J Struct Eng 2015;141(10):04014240.
[25] Zlokovic GM. Group theory and G-vector spaces in structural analysis. Chichester: Ellis Horwood; 1989.
[26] Healey TJ, Treacy JA. Exact block diagonalisation of large eigenvalue problems for structures with symmetry. Int J Num Meth Eng 1991;31:265–85.
[27] Zingoni A, Pavlovic MN. On natural-frequency determination of symmetric grid-mass systems. In: Ferguson NS, Wolfe HF, Mei C, editors. Structural dynamics: recent advances. Southampton: Institute of Sound and Vibration Research; 1994. p. 151–63.
[28] Zingoni A. An efficient computational scheme for the vibration analysis of high-tension cable nets. J Sound Vib 1996;189(1):55–79.
[29] Mohan SJ, Pratap R. A group theoretic approach to the linear free vibration analysis of shells with dihedral symmetry. J Sound Vib 2002;252(2):317–41.
[30] Mohan SJ, Pratap R. A natural classification of vibration modes of polygonal ducts based on group theoretic analysis. J Sound Vib 2004;269:745–64.
[31] Zingoni A. On the symmetries and vibration modes of layered space grids. Eng Struct 2005;27(4):629–38.
[32] Kaveh A, Nikbakht M. Decomposition of symmetric mass-spring vibrating systems using groups, graphs and linear algebra. Commun Num Meth Eng 2007;23:639–64.
[33] Zingoni A. On group-theoretic computation of natural frequencies for spring-mass dynamic systems with rectilinear motion. Commun Num Meth Eng 2008;24:973–87.
[34] Kaveh A, Nikbakht M. Improved group-theoretical method for eigenvalue problems of special symmetric structures using graph theory. Adv Eng Softw 2010;41:22–31.
[35] Zingoni A. A group-theoretic finite-difference formulation for plate eigenvalue problems. Comput Struct 2012;112/113:266–82.
[36] Zingoni A. Vibration analysis and structural dynamics for civil engineers: essentials and group-theoretic formulations. London: CRC Press/Taylor & Francis; 2015.
[37] Zingoni A. Insights on the vibration characteristics of double-layer cable nets of D_{4h} symmetry. Int J Solids Struct 2018;135:261–73.
[38] Zingoni A. Group-theoretic vibration analysis of double-layer cable nets of D_{4h} symmetry. Int J Solids Struct 2019;176/177:68–85. https://doi.org/10.1016/j.ijsolstr.2019.05.020.
[39] Kaveh A, Nikbakht M. Stability analysis of hyper symmetric skeletal structures using group theory. Acta Mech 2008;200:177–97.
[40] Kaveh A, Rahami H. An efficient method for decomposition of regular structures using graph products. Int J Num Meth Eng 2004;61(11):1797–808.
[41] Kaveh A, Koohestani K. Graph products for configuration processing of space structures. Comput Struct 2008;86:1219–31.
[42] Chen Y, Feng J. Improved symmetry method for the mobility of regular structures using graph products. J Struct Eng 2016;142:04016051.
[43] Kaveh A, Nikbakht M, Rahami H. Improved group theoretic method using graphs products, for the analysis of symmetric-regular structures. Acta Mech 2010;210:265–89.
[44] Kaveh A, Nikbakht M. Analysis of space truss towers using combined symmetry groups and product graphs. Acta Mech 2011;218:133–60.
[45] Kaveh A. Optimal analysis of structures by concepts of symmetry and regularity. Vienna: Springer; 2013.
[46] Zingoni A. Truss and beam finite elements revisited: a derivation based on displacement-field decomposition. Int J Space Struct 1996;11(4):371–80.
[47] Wohlever JC. Some computational aspects of a group theoretic finite element approach to the buckling and postbuckling analyses of plates and shells-of-revolution. Comput Meth Appl Mech Eng 1999;170:373–406.
[48] Zingoni A. Group-theoretic computation of matrices for rectangular hexahedral finite elements. In: Bathe KJ, editor. Proceedings of the first MIT conference on computational fluid and solid mechanics. Oxford: Elsevier Science; 2001. p. 1683–5.
[49] Zlokovic G, Maneski T, Nestorovic M. Group theoretical formulation of quadrilateral and hexahedral isoparametric finite elements. Comput Struct 2004;82(11/12):883–99.
[50] Zingoni A. A group-theoretic formulation for symmetric finite elements. Finite Elem Anal Des 2005;41(6):615–35.
[51] Kaveh A, Fazli H. Graph coloration and group theory in dynamic analysis of symmetric finite element models. Finite Elem Anal Des 2007;43(11/12):901–11.
[52] Suresh K, Sirpotdar A. Automated symmetry exploitation in engineering analysis. Eng Comput 2006;21(4):304–11.
[53] Zingoni A. Symmetry recognition in group-theoretic computational schemes for complex structural systems. Comput Struct 2012;94/95:34–44.
[54] Chen Y, Sareh P, Feng J, Sun Q. A computational method for automated detection of engineering structures with cyclic symmetries. Comput Struct 2017;191:153–64.
[55] Chen Y, Fan L, Feng J. Automatic and exact symmetry recognition of structures exhibiting high-order symmetries. J Comput Civil Eng (ASCE) 2018;32:04018002.
[56] Zingoni A. Group-theoretic exploitations of symmetry in computational solid and structural mechanics. Int J Num Meth Eng 2009;79:253–89.
[57] Zingoni A. Group-theoretic insights on the vibration of symmetric structures in engineering. Philosoph Trans Roy Soc A 2014;372:20120037.
[58] Zingoni A. On the most appropriate symmetry group for group-theoretic computational schemes in structural mechanics. Oral presentation at the thirteenth international conference on computational structures technology, 4–6 September, Barcelona, Spain, 2018.